JOURNAL
OF
GEOMAGNETISM
AND
GEOELECTRICITY

VOL. XIII NO. 1, 2

SOCIETY
OF
TERRESTRIAL MAGNETISM AND ELECTRICITY
OF
JAPAN

1961
TOKYO

JOURNAL OF GEOMAGNETISM AND GEOELECTRICITY

EDITORIAL OFFICE: Society of Terrestrial Magnetism and Electricity of Japan, Geophysical Institute, Tokyo University, Tokyo, Japan

The fields of interest of this quarterly Journal are as follows:

Terrestrial Magnetism	Aurora and Airglow
Atmospheric Electricity	The Ozone Layer
The Ionosphere	Physical States of the Upper Atmosphere
Radio Wave Propagation	Solar Phenomena relating to the Above Subjects
Cosmic Rays	Electricity within the Earth

The text should be written in English, German or French.

The Editors

Characteristics of Solar Energetic Particles which Excite Polar-Cap Blackouts

By Kenji SINNO

Hraiso Radio Wave Observatory, Radio Research Laboratories, Japan.
(Read Oct. 31, 1960; Received Nov. 7, 1961)

Abstract

Ejection and prapagation of the particles which excite abnormal ionization in the polar upper atmosphere are investigated from some statistical considerations on ionospheric data *f-min* and cosmic radio observation by riometer.

Relations between the flares and the polar-cap blackouts insist the trapping of particles into the cloud which would be responsible for the geomagnetic disturbances; that is, a part of the energetic particles ejecting from the flare propagate with relativistic velocity in interplanetary space along the twisted solar magnetic line of force extending to the earth and excite the S-type polar-cap blackouts having sudden onset within a few hours after flare; on the other hand, another part of the energetic particles ejecting from the flare is trapped into the cloud and is carried with rather low velocity, then the particles would reach the earth by leaking from the cloud and excite the G-type polar-cap blackouts having gradual onset about 10 hours before commencement of geomagnetic storms.

1. Introduction

Recently, new evidence of the high energy solar particles has been found from several studies. Anderson, et al. (1959) showed difinitely the existence of solar protons by means of balloon observations at Churchill. On the other hand, Shapley, et al. (1958) and Haura, et al. (1958) (1959) showed from analysis of *f-min* ionosphere data that the intense polar blackouts caused by enhanced inoization in lower ionosphere at polar cap regions occurs after an intense solar flare associated with type IV solar radio outbursts.

These evidences have also been identified by riometric observation of the galactic radio noise (Little et al. 1959, Reid et al 1959, Hultqvist 1959) and by observation of VHF polar circuits (Bailey 1957, 1959).

Many papers on this subject have now been presented from the experimental and theoretical points of view. Lately, Obayashi and Hakura (1960) pointed out the tendency that the polar blackout particles originating to the west of solar central meridian reach to the earth earlier than those from the east, and they explain this tendency under the conception that the particles tend to travel easily and speedily along the curved solar magnetic lines of force which are twisted towards the east (Biermann 1957, Parker 1958).

Here, the ejection and propagation of the solar particles responsible for the polar blackout events has been discussed upon the consideration of both the corpuscular cloud which moves along the straight path from the sun at a low speed and the particles which moves along the twisted solar magnetie lines of force at a high speed.

2. Sudden and Gradual Onset of Polar-Cap Blackouts

During the period from January, 1956, through December, 1960, fifty pre-*ssc* polar-cap blackouts were observed by means of *f*-min ionosphere data at Thule, Greenland (Geograph. 77.29 N, 69.10 W; Geomag. 89.0, 357.8, near the geomagnetic north pole) and at Resolute Bay, Canada (Geograph. 74.41 N, 94.55 W; Geomag. 88.9, 289.3, near the magnetic north pole), and also by riometric observation at various stations (Reid et al. 1959).

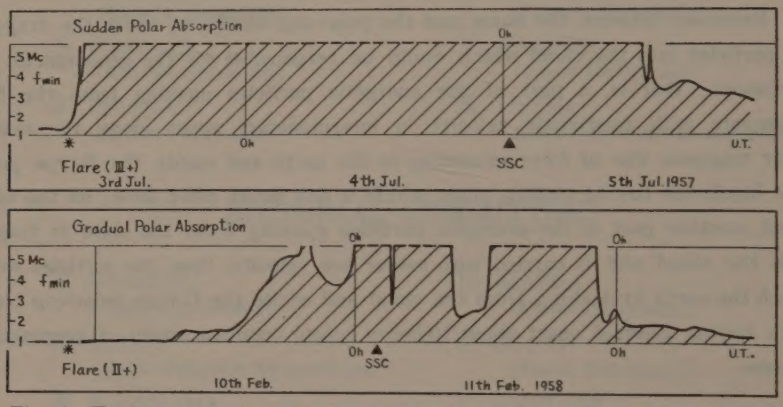

Fig. 1 Typical examples of polar blackout events observed by *f*-min of ionospheric data at Thule. The upper figure is Sudden-type event which started on 3rd July, 1957 and the bottom figure is Gradual-type event which started on 10th February, 1958.

The relevant details of these events have been compiled in Table I with their associated solar and magnetic events.

After looking over the development of the polar blackouts, we easily come to the conception that there are two types of polar-cap ionization events, one having a sudden onset within two hours (S-Type) and the other having a gradual onset (G-Type) (Sinno 1916 a).

The examples of S- and G-types of the polar blackouts observed from *f*-min ionospheric data at Thule are shown in Fig. 1.

3. Propagations of Polar Blackout Particles

3. 1 Propagation times between polar blackouts and geomagnetic disturbances

As has been investigated (Hakura et al. 1959), we can see from Table I that almost all cases of the polar blackout events are preceded, the same as the magnetic storms (Sinno et al. 1958), by type IV solar radio outbursts. Up to eighty percent of polar blackouts correspond to type IV outbursts from the table. The time delays of the

pre-*ssc* polar blackouts (Δt) and of the sudden commencements of geomagnetic storms (ΔT) after the flare are also tabulated in this table.

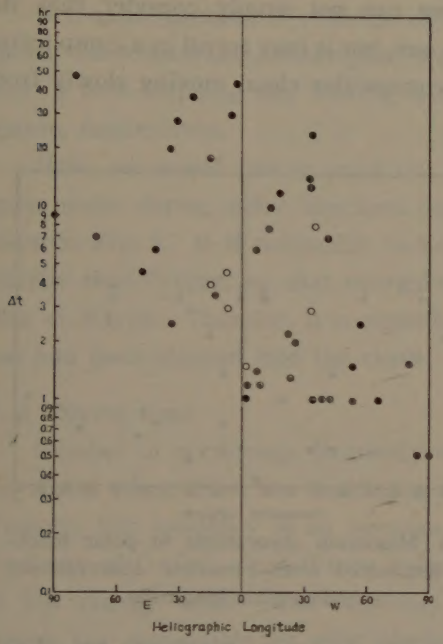

Fig. 2 Relation of the propagation time between polar blackouts Δt and magnetic storms ΔT. Polar-cap blackouts with sudden onset and gradual onset events are indicated by ⊙ and ●, resrectively, and uncertain events indicated by ○.

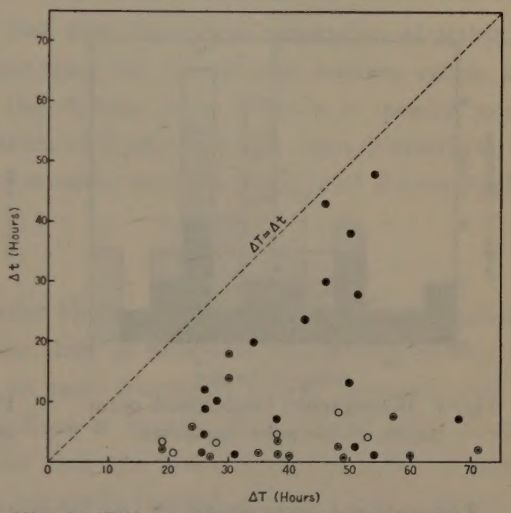

Fig. 3 Heliographic longitudinal distribution of the propagation times of polar blackout events.

The relation beween Δt and ΔT is shown in Fig. 2, indicating S and G-Types events as double circles and black circles, respectively, and uncertain type events as white circles. Remarkable characteristics we could easily deduce from Fig. 2 are the existence of two wings; one wing contains almost all S-type events starting within a few hours in Δt and the other wing contains almost all G-type events starting about ten hours before *ssc* (Sinno 1961a).

These characteristics lead to the conception that the latter shows some inter-relation with the corpuscular clouds responsible for the geomagnetic distubances. It may be suggested that a part of the energetic solar particles emitted from the flare is trapped into the cloud having a intense magnetic field and carried with it and then impinges into polar atmosphere by gradual leakage from the cloud.

3. 2 Heliographic longitudes

The time delays of the polar blackouts after the solar flares Δt are plotted in Fig. 3 according to their heliographic latitude. As was pointed out (Obayashi et al. 1960), the polar-cap blackouts are excited by the flares on the eastern side. These observed time-delays and western excess of the polar-cap blackouts are favorable to the conception that the solar magnetic line of force are twisted towards the east owing to the

solar rotation, since the particles easily propagate along the line of force. However, there are several events which belong almost to G-type as shown in Fig. 3, the travelling time corresponding to many hours, so we can not simply consider that the particle travels along the line of force from the sun, but it may travel in a complicated manner, e. g., the particle is trapped within the corpuscular cloud moving slowly from the sun before it leaks from the cloud.

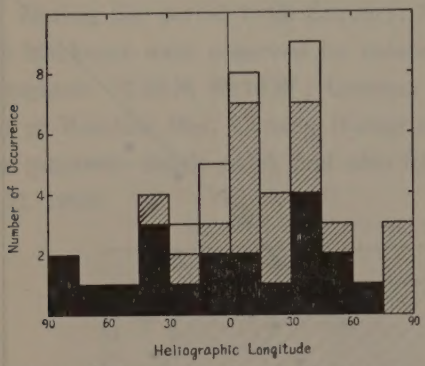

Fig. 4 Heliographic longitudinal occurrences of the polar blackouts.

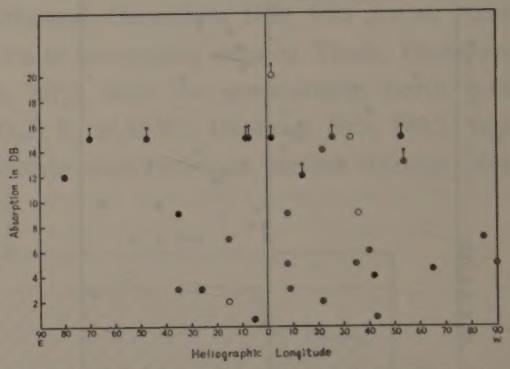

Fig. 5 Maximum absorptions of polar blackouts (estimated from riometric observations) vs heliographic longitude.

Longitudinal occurrences of the flares responsible for polar blackouts are shown in Fig. 4. We can find the significant west hemisphere excess in respect of S-type and also solar cosmic ray increase, as has been presented by Reid and Leinbach (1959) etc., but we see G-type blackouts correspond to the flare of rather wide spread longitudes.

We know that trapping of the energetic particles into the cloud is more effective by the flare of eastern heliographic longitude than those of western heliographic longi-

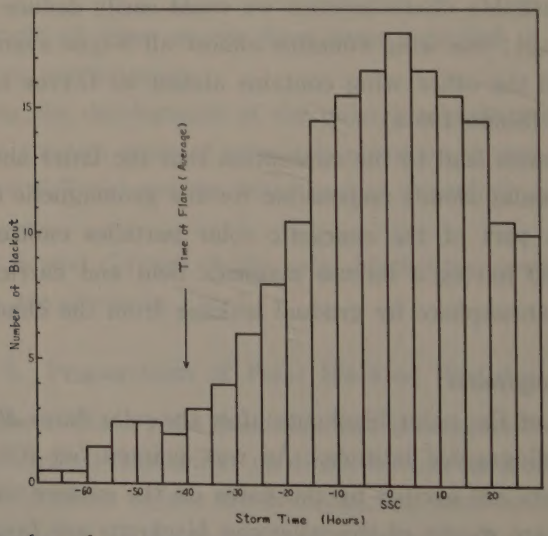

Fig. 6 Number of occurrences of polar blackouts with respect to the geomagnetic storm time.

tude, as shown by the present author from investigation of cosmic ray storms (Sinno 1961b).

If G-type blackout is evidence of leakage of the trapped energetic particles in the cloud, the widespread heliographic occurrence of G-type would be caused by combination of both trapping and leaking tendencies, predominating to east and west hemisphere, respectively.

Here, we would like to point out the fact that ionosphere absorption of galactic radio noise during polar blackout does not show the heliographic western excess, as show in Fig. 5. It is noticeable to know that G-type polar blackout is usually more intense than S-type, so that energy spectrum of G-type is much steep comparison to that of S-type. Therefor, it is plausible to consider that the particles of G-type blackout had been trapped into the cloud.

3. 3 Storm time

Number of occurrence frequency of polar blackouts with respect to the geomagnetic storm time takes the maximum at the time of near *ssc*, as shown in Fig. 6. Though, this tendency is an average of all polar blackouts, it may represent only a tendency of G-type, since G-type polar blackout is usually more intense than S-type in low energy range. The fact may show that the lower energy particles of solar cosmic ray responsible for polar blackouts are easily trapped into the cloud, compared with the higher energy particles of solar cosmic ray which reach their mamimum within a few hours after the flare, because the trapping ability may be inversely proportional to energy of the particles as has been discussed by the present author (Sinno 1961b). Thus, S-type polar blackout with sudden onset (~100 MeV as proton) might be a trace of unusual increase of solar cosmic rays since they have rather flat spectrum towards the higher energy. Actually, we have always observed S-type polar blackouts at the time of unusual solar cosmic ray increase.

3. 4 Ejections of Polar Blackout Particles

The fact that the polar-cap blackout phenomenon is excited by the major solar flare associated with the type IV radio emission was already confirmed statistically on the IGY data (Hakura et al. 1959, Thompson et al. 1960). It is also well known that the cause of the type IV solar radio outburst is synchrotron radiation from the relativistic electrons in the solar outer corona (Boischot et al. 1957). The existance of a large number of those energetic electrons leads us to the conception that there are also many protons with relativistic energy.

When these protons are ejected from the sun, the corpuscular cloud responsible for the geomagnetic storm and also the cosmic-ray storm should be ejected, since it is true that both the storms are excited by the solar flare associated with the type IV radio noise.

As we already known, big solar radio outbursts are usually consisted by two parts, pre-flare (first part) and post-flare (second part) outburst (Dodson et al. 1953). Pre-flare outburst is characterized by abrupt onset of outburst having very wide frequency ranges

and closely associated with *SID* phenomenon of ionospheric radio propagation. On the other hand, post-flare outburst called type IV, is characterized by gradual onset of outburst having rather low frequency below several hundred Mc, and closely connected with the cloud responsible for the geomagnetic storm and the cosmic ray storm (Sinno et al. 1958).

In order to answer the question of which part of the outbursts is evidence of the polar blackout particles, we will point out the following observational fact. We have several events where comic ray increase and S-type of polar blackout started before onset of post-flare outburst. That is, 23 rd February, 1956, pre-flare outburst started at 03 : 35, cosmic ray increase started before 03 : 50 and post-flare outburst started after 04 : 00. And, 12 th November, 1960, pre-flare outburst started at 13 : 21, cosmic ray increase and polar blackout started at about 13 : 40 and post-flare outburst started after 14 : 00.

On the other hand, we have also several events where G-type of polar blackout was excited appreciable pre-flare outburst (11 th September. 1957 and 9 th February, 1958).

Furthermore, we have a statical investigation which supports this correspondence, that is, the polar blackout having short propagation time corresponds to big solar outburst on higher frequencies (Sakurai et al. 1961), and to solar outburst with simultaneous onset over wide band (Sinno et al. 1958). The outburst having these characteristics should be the pre-flare outburst itself.

Then, we come to the conclusion that pre-flare outburst is the evidence of ejection of solar energetic particles and post-flare outburst is the evidence of trapping of the particles, though position of the flare may also have an important effect on excitation of polar blackout.

Table II Courses of Polar Blackouts

Flare (Location)	Solar Outburst (Ejection)	Interplanetary Space (Fropagation)	Polar Blackout (Phenomenon)
West Hemisphere	Pre-Flare	Along to Solar Magnetic Field	S-Type
	Post-Flare	Trapped into Cloud	G-Type
East Hemisphere	Pre-Flare	Along to Solar Magnetic Field	No Blackout

Courses of development of polar blackouts from solar flares are shown in Table II. If pre-flare solar radio outburst occurred in western heliographic longitudes, ejected energetic particles propagate along to the twisted solar magnetic line of force and could excite S-type of polar blackout and cosmic ray increase with short time delays, however if the same pre-flare outburst occurred in eastern or central heliographic longitudes, ejected particles propagate also along to the field and could not strike to the earth, then no polar blackout is excited. On the other hand, G-type polar blackout is excited by post-flare outburst occurring anywhere in visible heliographic longitudes,

since lateral dimension of the cloud is quite large as several A. U. near the earth orbit.

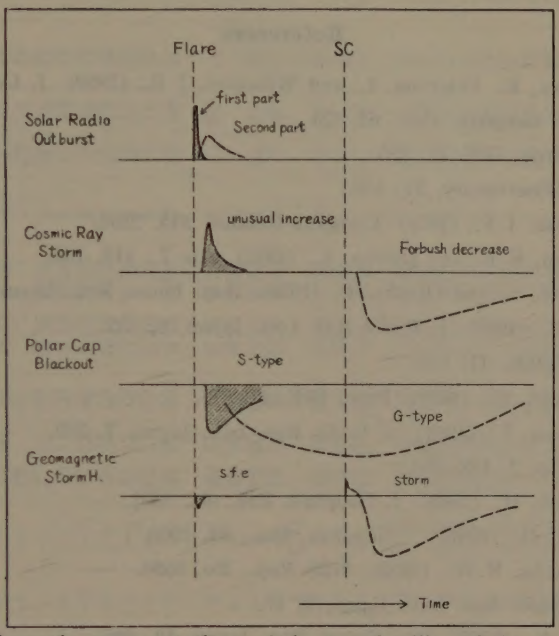

Fig. 7 Schematic representations of the two families of the earth storms.

Concluding Remarks

Ejection and propagation mechanisms of polar blackout particles are investigated from some statistical considerations.

It may be said that there are two ways of ejection of the energetic particles through association with either pre-flare or post-flare solar radio outbursts. The former particles having energy up to cosmic ray energies propagate speedily ($\sim 10^{10}$cm/sec) along to solar magnetic line of force twisted to the eastwards, and excite both S-type polar blackout with sudden onset and solar soft cosmic ray increase, if the earth comes across the path of the particles. On the other hand, the particles having comparatively low energies are trapped easily into the cloud and carried with rather lower velocity ($\sim 10^{8}$cm/sec) in interplanetary space and particles leaking from the cloud excite G-type polar blackout with gradual onset, if the earth comes across the path of the cloud.

Auroral particles during magnetic storm might be also a trace of those of lower energy ranges and impinge into the upper atmosphere only during a restricted period, because they are trapped strongly into the cloud by their low momentum.

In concluding, we come to a conclusion that earth storms might be divided into two families, one constructed by solar cosmic ray including S-type of polar blackout, *SFE* of geomagnetism and *SID* of radio propagation, associated with pre-flare (first part) solar radio outburst, and the other constructed by cosmic ray storm (Forbush decrease), G-type of polar blackout including aurora, geomagnetic storm and ionospheric storm, associated with post-flare (second part) solar radio outburst, as shown in Fig. 7.

The author wish to express his thanks to the members of the Cosmic-ray Research Committee in Japan for their valuable discussions.

References

Anderson, K. A., Arnory, R., Peterson, L. and Winckler, J. R., (1959) J. Geophys. Res., **64**, 1133.
Bailey, D. K., (1957) J. Geophys. Res., **62**, 431.
Bailey, D. K., (1959) Proc. IRE, **47**, 255.
Biermann, L., (1957) Observatory, **77**, 109.
Boischot, A. and Denisse, J. F., (1957) Comptes Rendus, **245**, 2194.
Dodson, H. W. Hedeman, E. R. and Owren, L., (1953) Ap. J., **118**, 169.
Hakura, Y., Takenoshita, Y. and Otsuki, T., (1958) Rep. Ionos. Res. Japan, **12**, 459.
Hakura, Y. and Goh, T., (1959) J. Radio Res. Lab. Japan, **6**, 635.
Hultqvist, B., (1959) Tellus, **11**, 332.
Little, C. G. and Leinbach, H., (1959) Proc. IRE, **47**, 315.
Obayashi, T. and Hakura, Y., (1961) J. Radio Res. Lab. Japan, **7**, 379.
Parker, E. N., (1958) Ap. J. **128**, 664.
Reid, G. C. and Leinbach, H., (1959) J. Geophys. Res., **64**, 1801.
Sakurai, K. and Maeda, H., (1961) J. Geophys. Res., **66**, 1966.
Shapley, A. H. and Knecht, R. W., (1958) NBS Rep., No. 5596.
Sinno, K., (1961a) J. Radio Res. Lab. Japan, **8**, 17.
Sinno, K. and Hakura, Y., (1958) Rep. Ionos. Res. Japan, **12**, 285.
Sinno, K., (1961b) J. Radio Res. Lab. Japan, **8**, 289.
Thompson, A. P. and Maxwell, A., (1960) Nature, **185**, 89.

List of polar cap ionization events with associated phenomena

Date	Geomagnetic Storm		Polar Cap Ionization								Solar Events					ΔT	Δt
			Ionogram				Riometer				Flare			Radio			
	Start	Grade	Start	Dur.	Tpye	Obs.*	Start	Dur.	Abs.	Obs.*	Start	Position	Imp.	Start	Type		
	th h m		th h m	h			th h m	h	DB		th h m			h m		h	h
1956																	
Feb.	19 02 : 21	m	—	—	—	—	—	—	—	—	16 18 : 05	N22 E10	2+	18 : 04	IV	56	—
Feb.	25 03 : 07	s	23 04 : 00	—	S	TH	—	—	—	—	23 03 : 34	N25 W85	3+	03 : 35	IV	49	0.5
Mar.	02 23 : 42	m s	—	—	—	—	—	—	—	—	29 —	—	—	22 : 24	IV	50	—
Apr.	30 01 : 38	m s	27 22 : 00	28	G	RE	—	—	—	—	27 21 : 00	N15 W34	2	20 : 54	IV	53	1.0
May	16 04 : 17	s	—	—	—	—	—	—	—	—	13 17 : 50	S18 W30	1	17 : 52	IV	58	—
May	20 06 : 38	m s	—	—	—	—	—	—	—	—	17 22 : 30	S24 W18	3	22 : 34	IV	56	—
Aug.	31 10 : 16	m	—	—	—	—	—	—	—	—	28 22 : 20	N16 E50	2	22 : 43	IV	60	—
Sep.	02 02 : 30	s	31 16 : 00	59	S	RE	—	—	—	—	31 12 : 28	N18 E12	3	12 : 31	IV	38	3.5
Nov.	09 20 : 30	m s	—	—	—	—	—	—	—	—	07 11 : 09	S16 E30	3	11 : 15	IV	57	—
Dec.	27 15 : 03	m	—	—	—	—	—	—	—	—	25 21 : 50	S16 W02	2	22 : 18	IV	42	—
1957																	
Jan.	21 12 : 35	s	20 23 : 00	72	G	TH	—	—	—	—	20 11 : 16	S25 W18	3	10 : 57	—	25	12
Feb.	23 18 : 07	m s	22 05 : 00	62	G	TH	—	—	—	—	21 16 : 05	N20 W33	(3)	—	—	50	13
Mar.	01 16 : 14	s	—	—	—	—	—	—	—	—	28 00 : 05	N18 W35	3	00 : 01	IV	40	—
Apr.	17 11 : 36	s	—	—	—	—	—	—	—	—	16 10 : 40	N31 E85	3−	10 : 47	IV	25	—
May	—	—	—	—	—	—	19 02 : 00	6	1	CO	—	—	—	—	—	—	—
Jun.	—	—	19 22 : 15	105	G	TH	22 10 : 00	—	—	—	19 16 : 08	N20 E46	2+	16 : 14	IV	—	6
Jun.	25 00 : 46	m s	continued	—	—	—	—	—	—	—	24 08 : 45	N22 W14	3	08 : 47	IV	16	—
Jun.	30 05 : 28	s	continued	—	—	—	—	—	—	—	28 07 : 00	N09 E28	3	07 : 17	IV	46	—
Jul.	02 08 : 57	s	continued	—	—	—	—	—	—	—	—	—	—	—	—	—	—
Jul.	05 00 : 42	m s	03 —	65	S	RE	03 11 : 00	46	6	CO	03 08 : 00	N13 W40	3+	08 : 37	IV	40	1
Jul.	19 13 : 44	m	—	—	—	—	—	—	—	—	16 17 : 42	S33 W28	1+	17 : 53	IV	68	—
Jul.	27 19 : 59	m	24 20 : 45	27	S	RE	24 20 : 15	11	2	CO	24 18 : 16	S24 W22	3	18 : 13	IV	74	2.2
Aug.	29 19 : 20	m s	29 05·····	38	G	TH	29 13 : 00	77	9	CO	28 09 : 14	S30 E35	3+	09 : 30	IV	34	19.8
Sep.	02 03 : 14	s	31 14 : 15	100	S	TH	—	—	—	—	31 12 : 59	N26 W03	3	13 : 09	IV	38	1.2
Sep.	04 13 : 00	s	continued	—	—	—	02 21 : 00	32	9	CO	02 13 : 13	S25 W36	3	13 : 10	IV	48	8
Sep.	13 00 : 46	s	12 09 : 30	19	G	TH	12 12 : 00	—	0.5	CO	11 02 : 45	N17 E05	3	03 : 00	IV	46	30
Sep.	22 13 : 45	s	21 21 : 15	—	S	TH	21 19 : 30	31	5	CO	21 13 : 32	N13 W08	3	13 : 30	IV	24	6
Sep.	29 00 : 16	s	—	—	—	—	26 23 : 15	29	2	CO	26 19 : 02	S26 E15	3	19 : 26	IV	53	4
Oct.	21 22 : 41	m	21 11 : 15	—	S	TH	21 07 : 00	13	5	CO	20 16 : 44	S26 W35	3+	16 : 46	IV	30	14
Nov.	26 01 : 55	m s	—	—	—	—	—	—	—	—	24 08 : 48	S15 E37	3+	09 : 03	IV	41	—
1958																	
Feb.	11 01 : 25	s	10 07 : 30	31	G	TH	10 07 : 00	—	>12	CO	09 21 : 08	S13 W14	2+	21 : 09	IV	28	10
Mar.	14 12 : 21	m s	11 10 : 00	22	G	TH	—	—	—	—	—	—	—	—	—	—	—
Mar.	—	—	14 16 : 45	27	S	TH	—	—	—	—	14 15 : 18	S23 W80	3	—	—	—	1.5
Mar.	25 15 : 40	m s	25 09 : 45	87	G	TH	25 22 : 30	96	12	FY	23 09 : 50	S15 E80	3+	10 : 02	—	54	48
Apr.	—	—	10 11·····	40	G	RE	10 11 : 30	30	3	CO	—	—	—	—	—	—	—
Jun.	07 00 : 46	m s	05 00 : 15	54	(G)	RE	—	—	—	—	04 21 : 47	N15 W58	1+	21 : 40	IV	(51)	(2.5)

Jul.	08 07 : 48	s	07 02 : 15	133	G	RE	07 02 : 30	86	>15	TH	07 00 : 39	N24 W02	3+	00 : 27	IV	31	1
Jul.	31 15 : 29	m	29 04 : 15	27	S	RE	29 04 : 05	22	0.7	TH	29 03 : 03	S14 W43	3	03 : 04	IV	60	1
Aug.	17 06 : 22	m s	16 07 : 30	69	G	RE	16 06 : 30	48	>15	TH	16 04 : 32	S14 W53	3+	04 : 38	IV	26	1.5
Aug.	22 02 : 27	m	21 15 : 45	18	G	RE	21 15 : 00	19	3	PB	20 (0043)	N19 E26	3	00 : 42	IV	50	39.0
Aug.	24 01 : 40	m s	22 16 : 00	59	S	RE	22 17 : 00	80	9	TH	22 14 : 17	N21 W08	3	14 : 40	IV	36	1.4
Aug.	27 03 : 03	m s	26 02 : 00	50	S	TH	26 01 : 00	71	>13	TH	26 00 : 05	N20 W54	3	00 : 19	IV	27	1
Sep.	16 09 : 30	m	—	—	—	—	—	—	—	—	14 08 : 32	S10 W74	3+	08 : 55	IV	49	—
Sep.	25 04 : 08	m s	22 16 : 00	72	(G)	TH	22 14 : 30	68	4	PB	22 07 : 41	S17 W42	2+	—	—	68	6.9
Oct.	24 07 : 31	m s	—	—	—	—	—	—	—	—	21 23 : 32	S03 W22	2	23 : 28	IV	56	—
Oct.	27 15 : 23	m s	—	—	—	—	—	—	—	—	24 14 : 41	S04 W56	3	14 : 43	IV	73	—
Dec.	15 20 : 22	m	—	—	—	—	—	—	—	—	12 12 : 32	S03 W09	2+	12 : 59	IV	80	—
1959																	
Feb.	14 11 : 42	m	—	—	—	—	—	—	—	—	12 23 : 00	N15 E55	3	23 : 03	IV	37	—
May	11 23 : 28	s	11 02 : 15	160	G	RE	11 01 : 30	190	>15	TH	10 20 : 50	N23 E47	3+	21 : 16	IV	26	4.5
May	15 07 : 03	m s	—	—	—	—	—	—	—	—	11 20 : 10	N08 E42	3+	20 : 23	IV		
											13 05 : 10	N22 E26	2+	05 : 12	IV	—	—
Jun.	11 09 : 19	m s	—	—	—	—	—	—	—	—	09 18 : 00	N17 E90	2	16 : 51	IV	26	—
Jul.	11 16 : 25	m s	10 09·····	—	G	TH	10 07 : 00	90	>15	CO	10 02 : 10	N22 E70	3+	02 : 09	IV	38	7
Jul.	15 08 : 02	s	continued	—	—	—	14 07 : 00	51	>15	CO	14 03 : 42	N16 E07	3+	03 : 37	IV	28	3
Jul.	17 16 : 38	s	continued	—	(S)	—	16 22 : 50	34	>15	CO	16 21 : 15	N08 W26	3+	21 : 20	IV	19	2
Aug.	20 04 : 12	m	19 10·····	23	G	TH	—	—	—	—	18 10 : 22	N11 W34	3	10 : 29	IV	42	24
Sep.	03 22 : 00	m s	—	—	—	—	—	—	—	—	01 19 : 10	N04 E90	1+	19 : 14	IV	41	—
Dec.	—	—	—	—	—	—	—	—	—	—	30 17 : 22	N09 E07	3	17 : 39	IV	—	—
1960																	
Jan.	13 18 : 59	m	13 16·····	17	G	RE	—	—	—	—	11 20 : 54	N22 E02	3	20 : 56	IV	46	43
Jan.	18 07 : 35	m	—	—	—	—	—	—	—	—	15 13 : 34	S20 W66	2	13 : 47	IV	66	—
Mar.	31 09 : 54	s	30 11·····	17	G	RE	—	—	—	—	29 07 : 05	N12 E31	3	07 : 00	IV	51	28
Mar.	31 21 : 42	s	31 09 : 15	—	S	RE	31 07 : 30	14	7	TH	30 15 : 20	N11 E15	2+	15 : 29	IV	30	18
Apr.	02 23 : 13	m s	01 10 : 00	62	S	RE	01 09 : 45	86	3	TH	01 08 : 45	N13 W09	3	08 : 48	IV	38	1.2
Apr.	06 16 : 35	m	05 14·····	12	(G)	RE	05 08 : 00	40	3	TH	—	—	—	—	—	—	—
Apr.	30 01 : 32	m s	28 04 : 00	15	S	RE	28 05 : 00	24	3	TH	28 01 : 30	S05 E34	3	01 : 16	IV	48	2.5
Apr.	30 12 : 13	s	29 08 : 30	50	S	RE	29 06 : 00	114	14	TH	29 04 : 43	N11 W22	3	<04 : 40	IV	31	1.3
May	—	—	04 11 : 15	5	S	RE	04 10 : 44	44	5	TH	04 10 : 15	N12 W90	3	10 : 15	IV	—	0.5
May	08 04 : 21	s	06 —	>45	—	RE	06 18 : 30	101	>15	TH	06 14 : 04	S10 E08	3+	14 : 14	IV	38	4.5
May	16 11 : 20	m s	13 06·····	23	G	RE	13 06 : 20	65	4.5	TH	13 05 : 22	N29 W65	3+	05 : 18	IV	78	1
May	28 10 : 19	m s	—	—	—	—	—	—	—	—	26 08 : 55	N12 W14	2+	09 : 09	IV	49	—
Jun.	04 02 : 50	m s	—	—	—	—	—	—	—	—	01 08 : 24	N28 E46	3+	08 : 37	IV	66	—
Jun.	27 01 : 46	m s	—	—	—	—	—	—	—	—	25 11 : 36	N20 E06	3	12 : 00	IV	38	—
Jun.	29 19 : 38	m s	—	—	—	—	—	—	—	—	27 21 : 40	N23 W23	3	21 : 46	IV	46	—
Aug.	16 14 : 09	m s	14 13 : 15	40	S	RE	—	—	—	—	14 05 : 35	N20 W13	3	05 : 17	—	57	7.6
Sep.	04 (02 : 30)	m s	03 09 : 30	~60	G	RE	—	—	—	—	03 00 : 40	N17 E90	3	01 : 02	IV	26	8.9
Nov.	12 13 : 48	s	—	—	—	—	—	—	—	—	11 (03 : 15)	(N30 E20)	(3+)	03 : 21	IV	34	—
Nov.	13 10 : 30	s	12 16 : 00	—	—	KR	12 15·····	42	>20	KR	12 13 : 27	N27 W02	3+	13 : 28	IV	21	1.5
Nov.	15 13 : 03	m s	—	—	—	—	—	—	—	—	14 02 : 46	N30 W32	3+	03 : 19	IV	34	—
Nov.	15 21 : 55	s	15 06 : 00	—	—	KR	15 05 : 00	—	15	KR	15 02 : 07	N26 W33	3+	02 : 21	IV	19	2.9
Nov.	—	—	—	—	—	—	21 (06)	—	5	KR	20 (20 : 17)	N25 W90	1	—	—	—	—

* CO ; College, FY ; Ft. Yukon, KR ; Kiruna, PB ; Point Barrow, RE ; Resolute Bay, TH ; Thule.

The Solar Geophysical Events of November 1960

By Tatsuzo OBAYASHI*

Arctic Institute of North America, Washington D. C.
(Read Feburuary 17, 1961; Received Aug. 1, 1961)

Abstract

A series of outstanding solar-geophysical events of November 1960 is described. Results obtained various measurments; solar phenomena, cosmic, rays, ionosphere, geomagnetism and aurorae are summarized and include a theoretical model of disturbances which appears to be consistent to date. It is shown that the events of November 1960 are unique in that they provide not only the information of solar particles up to cosmic ray energy ranges, but also the knowledge of existing interplanetary magnetic fields. Some important discoveries made in the events are also described briefly.

A series of events occurred during November 1960 which were undoubtedly the most outstanding and complicated solar-terrestrial phenomena in recent years. Three solar cosmic ray events were observed which were associated with intense solar flares. The geomagnetic storms that followed were extremely severe. The upper atmosphere was very disturbed, and displayed unusually bright aurora and airglow.

Major events which have been reported so far are listed in Tables 1 and 2. There were at least eight important solar flares which have been identified as the possible source of major terrestrial disturbances. All flares except on November 6, were originated from the same active region, the McMath Plage Region 5925, which passed the central meridian of the sun around November 12. Three of them, November 12, 15, and 20, produced energetic solar cosmic rays, detected at sea level. Three major geomagnetic storms occurred that were accompanied by large Forbush type decreases of cosmic rays. Solar phenomena, geomagnetic activity, and records of cosmic rays and ionospheric absorptions ($f_{\min}$) near the geomagnetic pole are illustrated in Fig. 1. Details of these phenomena are given in subsequent individual descriptions.

1. The Event of November 12-13, 1960

An intense flare started 13^h23^m on November 12 near the central meridian of the sun, which had an active region a few days earlier. The flare developed from 13^h25^m, and reached a maximum at 13^h30^m. An outburst of solar radio emission of spectral type II was observed between 13^h27^m to 13^h31^m at 200 Mc/s, and then a strong outburst of type IV (continuum radiation) followed, reaching a maximum from 13^h30^m to 13^h50^m, and fading out by 18^h00^m. The *Hα* intensity curve at McMath-Hulbert

* Present address: Ionosphere Research Laboratory, Kyoto University, Kyoto.

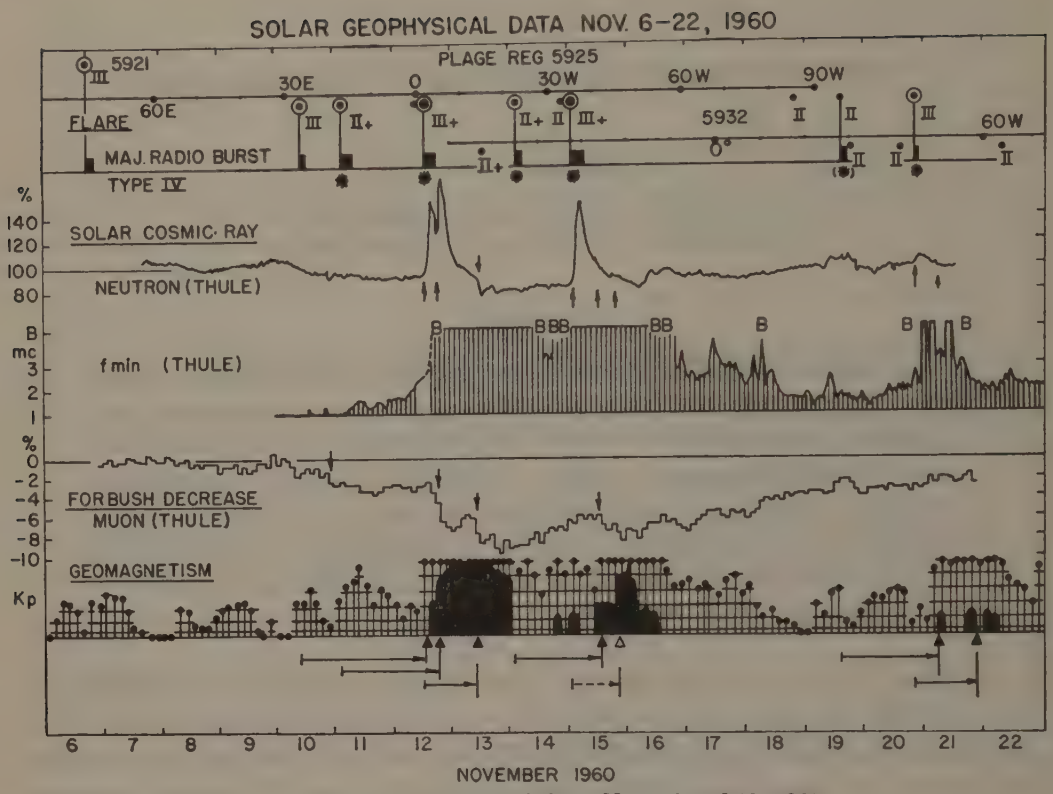

Fig. 1. Solar and geophysical data, November 6-22, 1960

Table 1 Major Events, November 6–22, 1960

Date	Flare		Radio Outburst		SWF (SID)		Cosmic Ray** Increase	
	Imp.	Time & position	Type	Time*	Imp.	Time	ΔI %	Time
6	III	1752–2030 07E 13N	Maj.$_+$	1827–1858	I	1708–1815	–	–
10	III	1011–1430 28E 29N	– Maj.$_+$	1020–1116 1116–1200	II	1022–1152	–	–
11	II$_+$	0305–0428 12E 29N	III II IV	0316–0330 0332 0340–0730	III$_+$	0311–0616	–	(PCA)
12	III$_+$	1323–1922 4W 26N	II IV	1327–1331 1330–1800	III$_+$	1325–1600	65 120	1340– 1900–1030 (13 th)
14	II$_+$	0246–0520 19W 27N	– IV	0318–0335 0335–0700	III	0300–0500	–	(PCA)
15	III$_+$	0207–0427 33W 26N	II IV	0221–0225 0225–0700	III$_+$	0220–0630	85	0240–22···
19	II	1543–1649 90W 28N	III (IV)	1559–1602 1636–1723	– –	– – –	–	(PCA)
20	III	2017–2024 (110W) 25N	II IV	2023–2035 2027–2046	III$_-$	2023–2145	5	2100–18··· (21 st)

* Time at 200 Mc/s.

** Deep River

Table 2 Major Events, November 6–22, 1960

Date	Geomagnetic Storm				Associated Cosmic Ray Forbush Decrease		Probable Origin Solar Flare	Delay Time hrs.
	Sc Mag. Time	Storm* (ΔH)av.	Main Phase Time	(ΔH)av.				
11	11-0033	12 γ	11-·····	110 γ	11-00···	M	6-1755 III	102.7
12–13	12-1348	42	12-17···	450	– –	–	10-1011 III	51.6
12–13	12-1846	36	12-19···		12-1930	S	11-0305 II_+	39.7
13–14	13-1021	(200)	13-11···	(250)	13-1035	S	12-1323 III_+	21.0
15–16	15-1304	22	15-17···	240	15-1330	M	14-0246 II_+	34.3
15–16	(15-2155)	(10)	15-22···		(15-2200)	(M)	15-0207 III_+	19.8
21–22	21-0632	15	21-07···	110	(21-06···)	(M)	19-1543 II	38.8
21–22	21-2147	20	22-00···	70	(21-22···)	(M)	20-2017 III	25.5

* Average of several low latitude stations, ΔH in gamma.

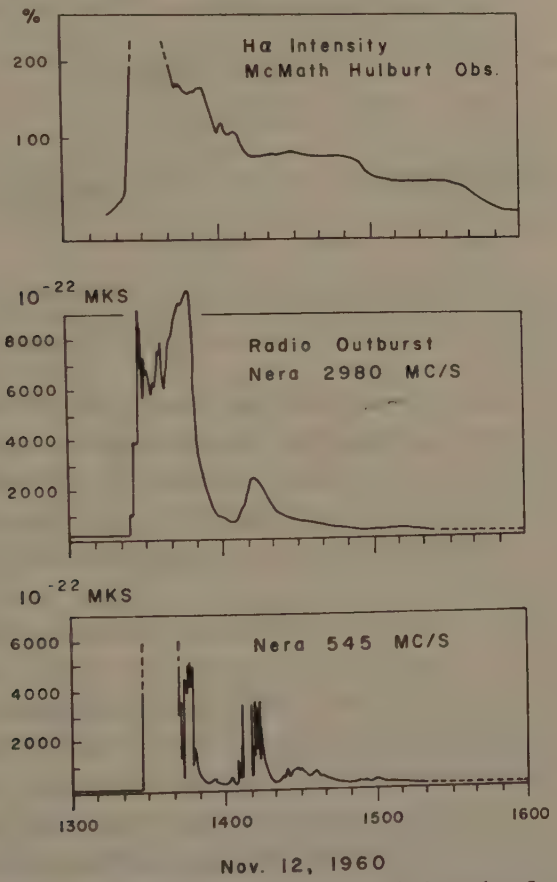

Fig. 2 Hα and radio outbursts records of the solar flare on November 12, 1960. (H. W. Dodson, and A. D. Fokker)

Observatory and radio outbursts at Nera, Netherlands, are reproduced in Fig. 2.

Tables 1 and 2: Information from Solar-geophysical Data, CRPL-F-B, NBS is included (Lincoln, 1961).

As has been pointed out by Dodson, the *Hα* record of this flare resembles closely that of cosmic ray produced flares such as February 23, 1956 and July 16, 1959. In fact, the most outstanding feature of this flare was the production of energetic solar cosmic rays. At $13h40m$, about 10 minutes after the onset of the major radio outburst of type IV, a distinct increase of the cosmic ray flux was observed at most neutron monitor stations in high latitudes. As shown in the record at Deep River, Canada, in Fig. 3, following a gradual rise, the flux intensity reached a maximum in about 2.5 hours and then decreased until a sudden rise occurred near $19h00m$. The second increase had a maximum at $20h00m$, exceeding 100 per cent above the normal level, and then a smooth recovery followed until about $10h30m$ on November 13.

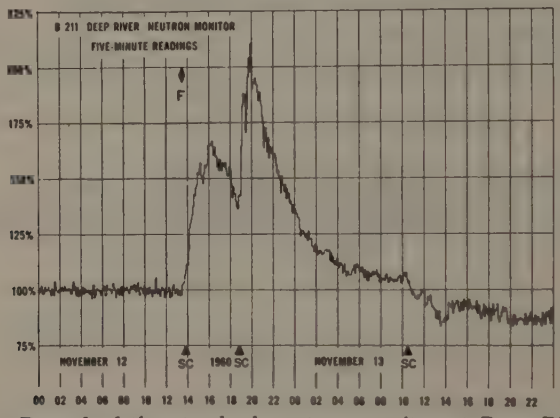

Fig. 3 Record of the standard neutron monitor at Deep River on November 12-13, 1960. (J. F. Steljes and H. Carmichael)

It has been noted that the solar flare and radio outburst intensities were substantially reduced after 15 *h*, and that there was no resurgence or new flare outbreak between 18 *h* to 20 *h* that could provide an obvious solar explanation for the second increase in cosmic rays. Therefore, the complex time variation of cosmic rays observed in this event must be understood in terms of the modulation effect upon the original flux of solar cosmic rays.

In this respect, geomagnetic storms which occurred in this period are of particular importance, because they provide the information of any existing solar plasma cloud in space, and of the outer geomagnetic field, where solar cosmic ray particles might interact and likely be modulated. In fact, two sudden commencements (*SC*) of geomagnetic storms were noticed in the earlier part of the event at $13h48m$ and $18h46m$ on Novemer 12. Magnetograms obtained at Hiraiso Radio Observatory are shown in Fig. 4. Unlike the first *SC* of the geomagnetic storm, the second one occurred right after the beginning of the main phase of the preceding storm. However, it was clearly seen in magnetograms obtained at most equatorial stations. Furthermore, a very sharp Forbush decrease of cosmic ray flux, which was observed in the meson monitor at MIT, followed soon after the second *SC*. Since almost all sudden Forbush decreases follow *SC*'s of geomagnetic storms within a few hours, it is rather convincing that the

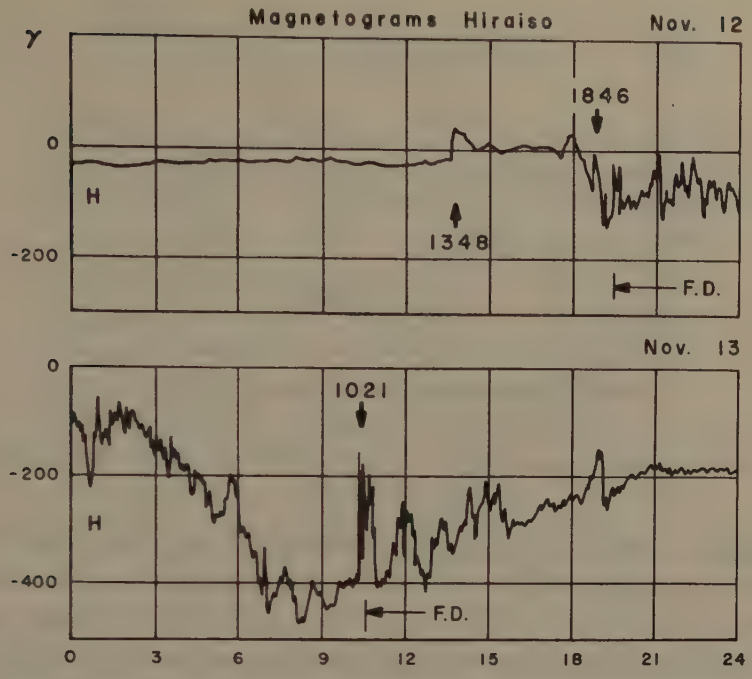

Fig. 4 Magnetograms of H-component observed at Hiraiso Radio Observatory, geomagnetic latitude 26 N, on November 12-13, 1960.

SC at 18*h*46*m* is a really important one. It should be noted that the second large increase of cosmic ray flux coincides at nearly the time of onset of a geomagnetic storm. As will be discussed later, this fact is essential in order to explain the complicated structure of this solar cosmic ray event.

As has been noted in Table 2, these *SC*'s probably originated from the earlier flares on November 10 and 11, respectively. Therefore, at the time of the flare of November 12, solar plasma clouds responsponsible for these storms were in the vicinities of the earth, but not yet enveloping it. It appears also reasonable to presume that a conspicuous sharp *SC* and a Forbush decrease at 10*h*21*m* on November 13 were caused 21 hours later by a plasma cloud ejected from the flare relevant to the solar cosmic ray event.

In the polar ionosphere, soon after the solar flare of November 12, the polar cap absorption event started, which was noted by riometers as well as vertical ionosondes. There was also some indication that a weak polar cap absorption had already been in progress near the geomagnetic pole as early as 01*h* on November 12 (Gregory 1961). However, a more pronounced increase of absorption was certainly started around 14*h* 00*m*. The riometer records at Cape Jones in Fig. 5, illustrate that the absorption at 30 Mc/s went up steadily and reached beyond the dynamic range (12db) by 18*h*. The 60 Mc/s riometers at Ottawa and Churchill, however, showed a sharp increase in absorption at approximately 19*h*00*m*, coinciding with the time of the second cosmic ray increase. Most other stations also showed similar time variation, indicating again

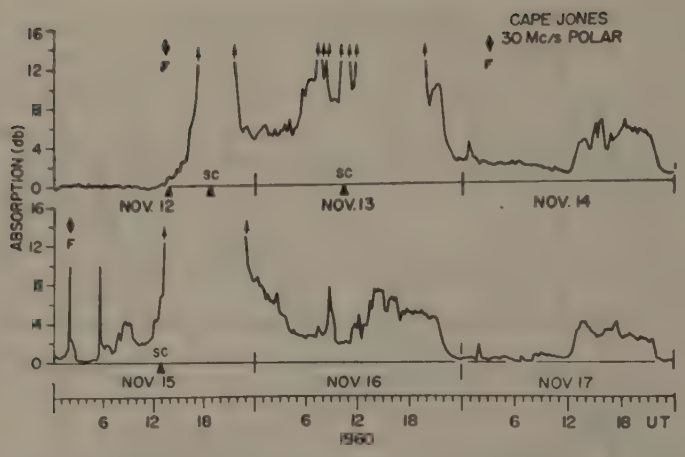

Fig. 5 30 Mc/s riometer record at Cape Jones on November 12–17, 1960. (E. L. Vogan)

a close association with the onset time of a geomagnetic storm (Vogan and Hartz, 1961).

It is generally accepted that polar cap absorptions are caused by the precipitation of low-energy solar cosmic rays of 10–100 Mev. High altitude balloon observations made by Minnesota University group and rocket measurements at Churchill by NASA in this event, revealed the existence of an enormous amount of low-energy solar cosmic rays. The result from the Explorer VII (Van Allen, 1961) also confirmed this. The estimated peak proton flux above 30 Mev exceeded 10^5 cm^{-2} sec^{-1} and the exponent of integral spectrum in this energy range would be approximately of −2 to −3.

Both polar cap and auroral absorption were extremely intense during the active phase of the geomagnetic storm of November 12-13, and a remarkable red aurora was seen as low as 40° geomagnetic latitude. The *F*-2 layer appeared to be completely wiped out during period of several hours, as indicated by ionosonde records and by lunar reflection experiments at Jodrell Bank and Sagamore Hill, Massachusetts.

2. The Event of November 15, 1960

A very similar, almost identical, intense flare was observed on November 15 at 02*h* 07*m*. Radio outbursts started 02*h*21*m* which appeared at type II, and then almost immediately a gradual build up of a type IV continuum followed from 02*h*25*m* to 07*h* 00*m*. The records of *Hα* intensity and of radio outbursts observed at Tokyo Astronomical Observatory and Hiraiso Radio Observatory are reproduced in Fig. 6.

The cosmic ray increase associated with this flare (Fig. 7, at Deep River, Canada) started very sharply near 02*h*40*m* and rose, in 15 minutes, to a rather flat, jagged top. A smooth recovery began about 05*h*00*m* at a rate similar to that of the event of November 12. Unlike the previous event, there was no *SC* of a geomagnetic storm until November 15 at 13*h*04*m*, and apparently the solar cosmic ray flux did not show any appreciable geomagnetic storm effect.

On the other hand, the polar cap absorption observed by the riometer at Cape Jones (Fig. 5) showed that a very gradual rise after the flare continued until the time of

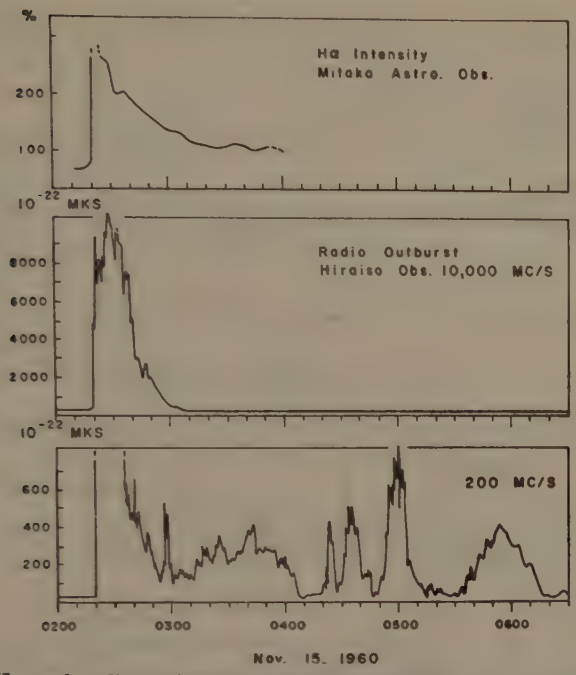

Fig. 6 Hα and radio outbursts records of the solar flare on November 15, 1960. (S. Nagasawa and F. Yamashita)

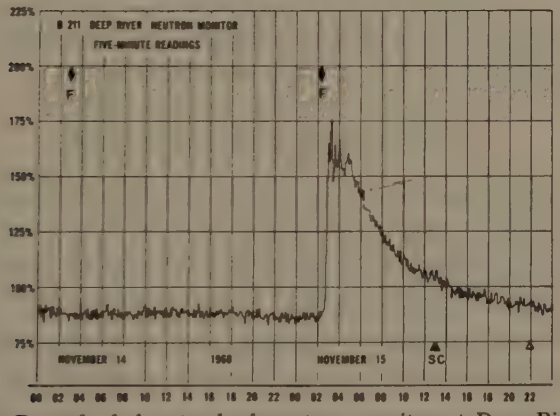

Fig. 7 Record of the standard neutron monitor at Deep River on November 14-15, 1960. (J. F. Steljes and H. Carmichael)

SC of the geomagnetic storm. At about 13*h*00*m* the absorption increased to very high values. Since there exists a marked sunrise effect in absorption, it is not certain whether the time variation of this polar cap absorption event well represents the change of solar cosmic ray flux in outer space, or the effect in the ionosphere itself.

Though a geomagnetic storm started at 13*h*04*m*, the magnetic activity was fairly moderate until 21*h*55*m* when a sudden outbreak of activity commenced (Fig. 8). This might have been the moment when the plasma cloud, emitted from the flare of November 15, arrived to the earth after a delay of about 20 hours. This geomagnetic storm was rather small compared with the one of November 12-13. Therefore, auroral

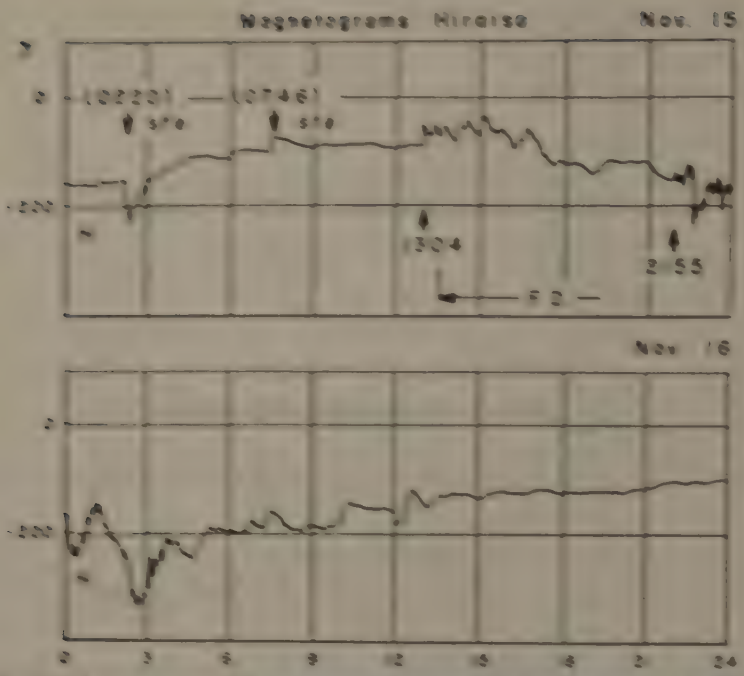

Fig. 8 Magnetograms in H-component observed at Hiraiso Radio Observatory, Japan on November 15-16, 1960.

and ionospheric disturbances were moderate and the southward extension of the auroral zone was not as remarkable as that of the previous storm.

3. The Event of November 20, 1960

Around November 14, the active region 3600 had turned around the western limb of the solar disk and yet the third cosmic ray increase was observed at 1140Tw on November 20. In fact, a spectacular limb flare was observed, coinciding with the time of the cosmic ray event. As shown in Fig. 9, this flare appeared about 2040Tw as a small mound on the limb, and then a sudden outbreak of brightness occurred between 2047Tw to 2049Tw (Jensen, 1961). The flare was certainly beyond the limb, and its position has been estimated by Warwick (1961) to be about 20° off the west limb. A strong radio outburst of continuum radiation accompanied the flare from 2047Tw to

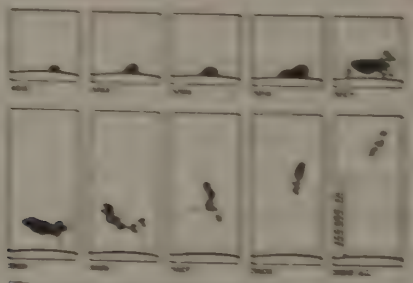

Fig. 9 The solar limb flare on November 20, 1960. West limb, 25° North. (R.T. Hansen)

$20h46m$. During this period, a remarkable ascending prominence was seen above the limb with a velocity of the order of a thousand km/sec.

A distinct yet very small cosmic ray increase began at about $21h00m$, which was a delay of about 30 minutes after the start of the radio outburst (Fig. 10). The rise time of approximately one hour, was comparatively slow, and after $23h00m$, a gradual decay followed until around 18 h on November 21. This is the first solar cosmic ray event whose source has been identified outside the visible solar disk.

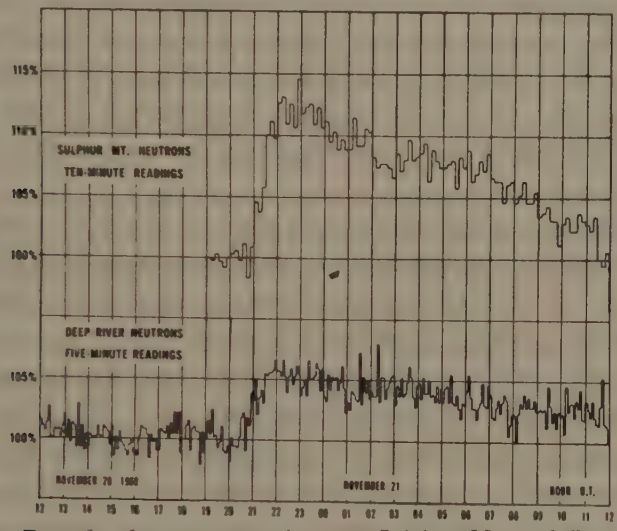

Fig. 10 Records of neutron monitors at Sulphur Mt. and Deep River on November 20-21, 1960. (H. Carmichael, J. F. Steljes, D. C. Rose and B. G. Wilson)

Theoretical Interpretations of the Events

The most outstanding feature of the November events is the emission of energetic solar cosmic rays. Three of the events, November 12, 15, and 20, involved particles above the relativistic energies. There are some good reasons to believe that the flares on November 11, 14, and 19, produced the particles of sub-relativistic energies (low-energy solar cosmic rays).

It has been known that most solar cosmic ray events are closely related to intense solar flares associated with type IV solar radio outbursts. In this respect, it is consistent that all type IV outbursts observed in this period were followed either by the cosmic ray increase of relativistic energies or by the polar cap absorptions, which is presumably produced by the particles of 10–100 Mev. Since type IV outbursts are believed to be the synchrotron radiation from relativistic electrons spiralling in magnetic fields, it is also likely that such agitated solar plasma bearing magnetic fields may be capable of accelerating solar protons from thermal to very high energies. However, it is not yet clear why only three of them produced relativistic solar cosmic rays. As has been stated by Dodson (1961), the flare of November 12 and 15 had very distinct features among other intense flares; they show the development, after flare maximum, of a very

complex loop-type prominence of absorption features and of large coverage of the nearby spots by a structureless extensive glow. The flare of November 15 was also seen by the naked eye in pearly white color, which might be of the synchrotron origin (Nagasawa et al, 1961). These facts are very encouraging for further studies of this problem.

The time variation of cosmic rays on November 12 is unusual among other solar cosmic ray events in the past. The feature of double peaks is of particular interest because of its unique shape. As has already been pointed out, any obvious solar origin as the cause of this variation was ruled out since there was no resurgence or a second flare which might provide a new source for the second increase of cosmic rays. Therefore, the time variation of solar cosmic rays on November 12 must be understood by means of the modulation of flux in interplanetary space or in the outer geomagnetic field.

Since a geomagnetic storm started soon after the flare, a depression of the geomagnetic cut-off owing to the distortion of the field may cause an increase of incoming cosmic ray flux to the earth (Ionosphere and Radio Astronomy, Nera, P. T. T., 1961; Kodama and Kitamura, 1961). However, it is rather difficult to conceive the fact that a large second increase was also observed at Thule, near the geomagnetic pole where the effect is expected to be very scarce (Pomerantz, 1961). Hence, this mechanism may explain a part of the increase observed at latitudes outside the polar cap, but certainly not be responsible for the substantial part of the second cosmic ray increase. Thus, the modulation of cosmic ray flux must be taking place somewhere in outer space beyond the geomagnetic field.

The argument follows that magnetic plasma clouds existing in the interplanetary space, play an impartant role in the modulation of solar cosmic rays. It has already been suggested by Gold (1959, 1961) that the solar plasma cloud ejected from the flare, may draw out any magnetic field existing in the vicinities of the sun, since the cloud itself has a high conductivity. As the plasma cloud advances into interplanetary space, it must form an expanding shell or a bulge of magnetic lines of force, such as shown in Fig. 11a. Supposing that solar cosmic ray particles are injected into this magnetic

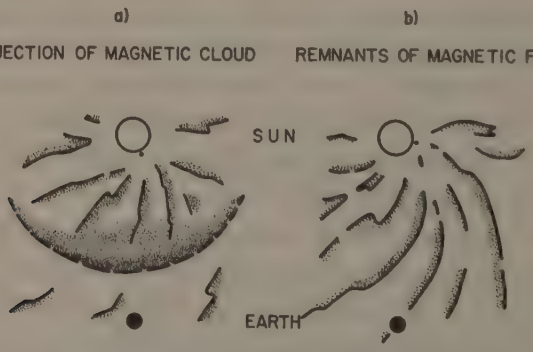

Fig 11 Schematic diagrams of the interplanetary magnetic fields:
a) Magnetic cloud associated with a solar eruption.
b) Remnants of magnetic fields.

bulge, then most particles are trapped inside by magnetic field lines, and advance in interplanetary space essentially with the same speed as the front of a cloud but not with the speed of the particle itself. When such a magnetic cloud evolves about the earth, which is indicated by the onset of a geomagnetic storm, a substantial rise of solar cosmic ray flux is expected. On the other hand, a magnetic cloud will also act equally to exclude the cosmic ray particles coming from outside the solar system, which may be identified as the so-called Forbush decrease of cosmic rays.

The event of November 12 was exactly the same situation as described above. According to Steljes, Carmichael and McCracken (1961), the flare shot out solar cosmic ray particles when two magnetic clouds, which were presumably produced by earlier flares, were advancing in the vicinity of the earth but not yet enveloping it. Judging from the onset of two *SC*'s of geomagnetic storms, their distances *from* the earth at the time of particle injection were 10^6 km and 2×10^7 km (1 *A. U.*$=1.5\times10^8$ km), respectively. Since the first *SC* was not followed by an appreciable Forbush decrease, it might be little magnetic field associated with it. However, the second one had a strong field so that it induced a large Forbush decrease.

The majority of solar cosmic ray particles ejected from the sun were stopped by the inner (second) magnetic cloud, and were trapped. However, a part of the particles, presumably high energy ones, would leak out through the magnetic barrier and reach the earth before the arrival of the magnetic cloud. A slow rise and subsequent fall of observed cosmic ray flux can be explained by this mechanism. The maximum energy of particles produced the first part of the increase would be 5 Bev. The integral spectrum was undoubtedly very steep (approximately E^{-4}).

Immediately after the arrival of the second magnetic cloud, a very sharp rise of particle flux was attained. Although the rise was steep, the increase was simultaneously world-wide, and there was no impact zone effect because the particles had already well migrated from the entire magntic cloud. The large Forbush decrease, observed after 19*h*30*m* by meson monitors, certainly indicated that the earth entered within the magnetic cloud in which cosmic ray particles coming from the outside of the cloud were excluded. During the period of this second increase, the low energy solar cosmic rays became abundant. This was detected by rocket and balloon measurements.

The time variation of polar cap absorption followed very similar pattern having two steps of the increase coinciding with the arrival of the magnetic clouds. This can be explained consistently by the trapping mechanism of solar particles, though the energy range relevant to this is of 10–100 Mev, considerably less than that detected by neutron monitors at sea level.

The flare of November 12, which produced this cosmic ray event, also ejected its own magnetic plasma cloud. The cloud arrived at the earth 21 hours later, and induced an extremely sharp *SC* and a sudden Forbush decrease as well. Although the *SC* occurred during a very active phase of the previous geomagnetic storm, the sudden impulse was noticeably recognized all over the world. It was of considerable interest that the solar cosmic ray flux suddenly disappeared after the arrival of this plasma

cloud. It has deen found by Roederer et al (1961) that, by examining the energy spectrum of incoming particles, the steep spectrunm characteristic for solar cosmic rays disappeared and a shallow spectrum remained which is common for galactic cosmic rays.

This fact indicates further support of the existence of the third magnetic cloud. Solar cosmic ray particles remained in interplanetary space were swept out by this magnetic cloud. It is quite possible that in front of the sweeping magnetic cloud, solar particles may be piled up. This was found to be the case since the polar cap absorption showed a sharp increas just before the *SC* of the geomagnetic storm.

On November 15, there was another increase of solar cosmic rays associated with an intense flare with a strong type IV radio outburst. Unlike the previous one, this had a much sharper increase and attained a single maximum within an hour. There was no geomagnetic storm until late on November, 15. However, at the time of the flare, the effect of Forbush decreases produced by previous magnetic clouds was not yet recovered. Thus, the earth was still within the huge magnetic cloud, and was connected directly to the sun by fairly well-ordered magnetic lines of force, as illustrated in Fig. 11b. Any particles ejected from the flare should be able to reach the earth quickly by spiralling down such lines of force. Also, their impact zones may be well-defined since the lines of force would direct and collimate the particles. In fact, McCracken (1961) has revealed that there was a discrete impact zone, and the particles were coming apparently from the direction of about 50° to the west of the sun-earth line.

Nevertheless, there is a puzzling fact. An *SC* of geomagnetic storm occurred at 13*h*04*m* on November 15. Judging from its delay-time, the plasma cloud responsible for this storm should have originated from the flare at 02*h*46*m* on November 14. If so, the plasma cloud was about 1/3 A. U. from the earth in the sun-earth line at the time when the solar cosmic ray particles were injected. Therefore, solar particles must have encountered this cloud before reaching the earth. The time variation of polar cap absorption did show some indication of this effect; a very slow rise of absorption until about the onset time of the geomagnetic storm. However, no appreciable effect was seen in the records of neutron monitors. It might be that the magnetic field in the plasme cloud was very weak, since the Forbush decrease associated with this geomagnetic storm was comparatively small. Therefore, the plasma cloud was rather transparent for cosmic ray particles, but still had enough magnetic fields to interact and trap low-energy solar cosmic ray particles.

The November 20 event provides still another interesting fact. The ejection of solar cosmic ray particles has a fairly wide angular spread from the source, and an appreciable amount of particles can arrive beyond the visible solar disk. However, this statement may be valid only for the case of the flare in the western limb. Of course, statistically, it seems to be likely that solar cosmic ray events are larger for the source near the central meridian.

It may also be worthwhile to note that the delay-time of geomagnetic storms,

which originated from the cosmic ray producing flares, was unusually short—21, 20 and 26 hours, respectively, for the present three cases. Further, these geomagnetic storms occurred while the preceding storms were still in the very active phase. There is some statistical evidence that, when two plasma clouds are ejected from the sun one after another, the second cloud travels at a much faster speed than the first one (Obayashi, 1961). This might be related to some complicated situation in the interplanetary magnetic fields, although a suitable explanation has not yet appeared.

Several interesting discoveries related to the November events have also been reported. A strong enhancement of molecular nitrogen bands, especially the first negative band of N_2^+, 3914Å had been detected in the polar cap region during the polar cap absorption events. Sandford (1961) has shown that the luminosity curve at 3914Å was very similar to that of the level of the polar cap absorption, essentially starting right after the solar flare. The variation was very steady, reaching a maximum approximately one-hundred times above normal at onset time of the geomagnetic storm, and then decaying to normal levels over the next two days. It appeared as an extensive glow rather than discrete auroral forms. The source of the emission exists at an altitude of 100 km or below, and it seems likely that it is excited by incoming solar cosmic ray particles.

Anomalous propagation of VLF radio waves has been confirmed during these solar cosmic ray events. It is believed that the radio waves propagate via an ionized layer formed by incident solar cosmic rays well below the ionosphere (Belrose and Ross, 1961; Ortner, Egeland and Hultqvist, 1961).

The material recovered from the Discoverer XVII, which was exposed to the solar cosmic ray event of November 12, has been under very careful study. An analysis by Yagoda and his group (1961) shows that there is a considerable abundance of radio isotopes produced by the impact of energetic particles, which is presumably by solar cosmic ray particles. A large amount of tritium content was also found. Since the observed ratio of tritium to argon 37 is much larger than that expected from the experiment of particle bombardments, Fireman (1961) has suggested that production of the large tritium content is not from the bombardment by solar protons, but from tritium in the flare itself.

Severe geomagnetic disturbances during the November events have offered the opportunity of investigating the geomagnetic storm effect on the air density of the upper atmosphere as revealed by the orbital motion of satellites. Jacchia (1961) and Grove (1961) found that appreciable increases of air density at the 200 km level occurred on November 13 and 15-16, which coincided with two maxima of the geomagnetic activity.

Several other prominent features in the November events are strong absorptions in VHF ionospheric scatter propagation in the polar region, hydrogen emission in auroral spectra, and formation of remarkable auroral red arcs. Such phenomena seem to be associated with unusual severe disturbances during this period.

Acknowledgements

The major part of this report is the résumé of the Conference on November 1960 Solar-terrestrial Events, which was held at the AF Cambridge Research Laboratories, Massachusetts, U. S. A., on February 15-17, 1961. The conference was organized by J. Aarons and S. Silverman of the AF Cambridge Research Laboratories, and the author, representing the Arctic Institute of North America.

The author wishes to express his thanks for all those who made important contributions at the conference, and also to Mr. Norman J. Oliver and his staff at the Ionospheric Physics Laboratory, AF Cambridge Research Laboratories, Dr. K. G. Mc Cracken, Massachusetts Institute of Technology for their kind collaborations.

This work has been sponsored by a U. S. National Science Foundation grant to the Arctic Institute of North America, Grant No. 13840.

References

Belrose, J. S. and Ross, D. B. (1961) Observation of unusual LF propagation during polar cap disturbancs, Read at the International Conference on Cosmic Rays and the Earth Storm, Kyoto, Sept., 1961.

Carmichael, H. and Steljes, J. F. (1961) Deep River Neutron Monitor Data, Atomic Energy of Canada Ltd., Chalk River, Canada.

Carmichael, H., Steljes, J. F., Rose, D. C. and Wilson, B. G. (1961) A solar cosmic ray increase on 20 November 1960, Phys. Rev. Letters **6**, 49.

Davis, L. R. and Ogilvie, K. W. (1961) Solar cosmic rays during the November 12, 1960 event, Read at the Meeting on the November Solar Event, NASA, Jan., 1961.

Dodson, H. W. (1961) McMath-Hulbert Observatory observations of the cosmic ray flare 1960, November 12, Read at the Meeting on the Solar-terrestrial Events of November 1960. AF-CRL, Feb., 1961.

Fireman, E. L. (1961) Tritium in the solar flare of November 12, 1960, Read at the Meeting on the Solar-terrestrial Events of November 1960, AF-CRL, Feb., 1961.

Gold, T. (1959) Plasma and magnetic fields in the solar system, J. Geophys. Res., **64**, 1665.

Gold, T. (1961) Recent evidence concncerning magnetic fields and particle fluxes in the solar system, Read at the Meeting of the American Geophys. Union, Washington D. C., April, 1961.

Grove, G. V. (1961) Correlation of upper atmosphere air density with geomagnetic storm activity, Read at the Meeting on the Solar-terrestrial Events of November 1960, AF-CRL, Feb., 1961.

Gregory, J. B. (1961) Antarctic observations of the solar proton events November 11-23, 1960, Read at the Meeting on the Solar-terrestrial Events of November 1960, AF-CRL., Feb., 1961.

Hansen, R. T. (1961) Cosmic ray flare of November 20, 1960, Phys. Rev. Letters **6**, 261.

Ionsphere and Radio Astronomy Section, P. T. T. Nera, (1961) The cosmic ray flare on Nov. 12, 1960 and solar activity during the period 10-15 Nov. 1960, Nature, **189**, 438.

Jacchia, L. (1961) Upper atmosphere air density variations during November 1960, Read at the Meeting on the Solar-terrestrial Events of November 1960. AF-CRL. Feb., 1961.

Kodama, M. and Kitamura, M. (1961) Some features of November 1960 events as inferred from cosmic rays, Read at the II nd International Space Science Symposium, Florence, Italy, April, 1961.

Landmark, B. (1961) Riometer and VLF observations at Norway, Read at the Meeting on the

Solar-terrestrial Events of November 1960. AF-CRL, Feb., 1961.

Lincoln, V. (1961) Solar-geophysical data, CRPL-F-B., NBS. November, 1960.

Nagaswa, S., Takakura, T., Tsuchiya, A., Tanaka, H. and Koyama H. A very unusual flare on November 15, 1960, Publ. Astro. Soc. Japan, **13**, 129.

Ney, E. P. and Stein, W. (1961) Solar cosmic rays in November 1960, Read at the International Conference on Cosmic Rays and the Earth Storm, Kyoto, Sept., 1961.

McCracken, K. G., (1961) The Propagation of cosmic rays through interplanetary space on May 4, 1960 and during November 1960, Read at the International Conference on Cosmic Rays and the Earth Storm, Kyoto, Sept., 1961.

Obayashi, T. (1961) Propagtion of solar corpuscles and interplanetary magnetic fields, Arctic Inst. North America, Research Rep. No. 16., and J. Geophys. Res., **67**, May, 1962.

Ortner, J., Egeland, A. and Hultqvist, B. (1961) The great earth storms in November 1960 as observed at Kiruna Geophysical Observatory, Kiruna Geophys. Obs. Sci. Rep. No. 1, Feb., 1961.

Pomerantz, M. A. (1961) Cosmic ray increases at Thule during November 1960, Read at the Meeting on the Solar-terrestrial Events of November 1960, AF-CRL., Eeb., 1961.

Roederer J. G., et al. (1961) Cosmic ray phenomena during the November 1960 solar disturbances. J. Geophys. Res., **66**, 1603.

Sandford, B. P. (1961) Polar glow aurora in polar cap absorption events, Arctic Institutte North America Research Paper, Aug., 1961.

Sheridan, K. V. and Trent, G. H. (1961) Spectral observations of two major solar outbursts in the frequency range 15 to 210 Mc/s Read at the Meeting on the Solar-terrestrial Events of November 1960, AF-CRL., Feb., 1961.

Steljes, J. F. Carmichael, H. and McCracken, K. G. (1961) Characteristics and fine structure of the large cosmic ray fluctuations in November 1960, J. Geophys. Res., **66**, 1363.

Thompson, A. R. (1961) Solar radio burst of 1960 November 12, Read at the Meeting on the Solar-terrestrial Events of November 1960, AF-CRL., Feb., 1961.

Taylor, G. N., and Whitney H. E., Klobuchar, J. A., (1961) Lunar reflection experiments between Jodrel Bank and Sagamore Hill, Mass. Read at the Meeting on the Solar-terrestaial Events of November 1960, AF-CRL., Feb., 1961.

Van Allen J. A., (1961) Preliminary survey of Explorer VII observations of solar cosmic rays 12-23 November 1960, Read at the Meeting on the November Solar Event, NASA., Jan., 1961.

Vogan, E. L. and Hartz, T. R., (1961) Ionosphere absorptions on November 1960, Canadian J. Phys. in the press. Read at the Meeting on the Solar-terrestrial Events of November 1960, AF-CRL., Feb., 1961.

Warwick, C. S. (1961) Summary of solar radio and optical observations 9-22 November 1960, Read at the Meeting on the Solar-terrestrial Events of November 1960, AF-CRL., Feb., 1961.

Winckler J. R. (1961) Balloon observations of solar cosmic rays during November 1960, Read at the Meeting on the November Solar Event, NASA., Jan., 1961.

Yagoda, H., (1961) Radiation studies of nuclear emulsions recovered from polar satellite orbits, Read at the Meeting on the November Solar Event, NASA., Jan., 1961.

Geomagnetic Storm Effects on Charged Particles

By Tatsuzo OBAYASHI

Ionosphere Research Laboratory, Kyoto University.
(Read Sept. 4; 1961; Received Nov. 7, 1961)

Abstract

The entry of high energy charged particles is studied taking into account the effect of field distortion due to a geomagnetic storm. By using a modified version of Störmer's theory, the cut-off rigidities of incoming particles are computed for two models of the outer geomagnetic field. The result is compared with the observed effect on precipitation of solar and galactic cosmic rays during the initial and main phases of a geomagntic storm.

Introduction

Charged particles entering from outside the earth are always affected by the outer geomagnetic field. Recently it has become evident that the upper atmosphere is exposed to various solar and cosmic particles of a wide energy spectrum ranging from a few Kev. up to relativistic energies. The precipitation of low-energy solar cosmic rays has been investigated by high altitude balloon observations (Winckler and Bhavsar, 1960; Winckler, Bhavsar and Peterson, 1961), and by analyzing world-wide ionogram data (Obayashi and Hakura, 1960). The results have shown that the variations of solar cosmic ray flux, in time as wll as in space, are very sensitive to distortion by the outer geomagnetic field, particularly during the main phases of geomagnetic storms. It has also been revealed that galactic cosmic rays tend to increase at low latitudes during a severe geomagnetic storm, although the time variation is usually superposed on the Forbush type decrease (Kondo, Nagashima, Yoshida and Wada, 1960).

A tentative calculation of the particle precipitation into the distorted geomagnetic field was made (Obayashi, 1959; Obayashi and Hakura, 1961). It has been concluded that the shift of polar blackouts towards the equator as well as the storm-time cosmic ray increases during geomagnetic storms are explained consistently by the lowering of the geomagnetic cut-off for incoming particles. The present paper is an extension of the previous study and emphasizes that the theory can account for the effect of particle precipitation, not only in the main phase, but also at the initial phase of a geomagnetic storm.

Theoretical Considerations

Following the previous paper (Obayashi and Hakura, 1961), the geomagnetic field is postulated as having a potential combining a dipole field of moment M and a

uniform field ΔH coinciding with the direction of the dipole axis. Using polar coordinates (r, θ, ϕ), the field components H_r and H_θ are expressd as

$$H_r=-\left(\frac{2M}{r^3}-\Delta H\right)\cos\theta \qquad (1)$$

and

$$H_\theta=-\left(\frac{M}{r^3}+\Delta H\right)\sin\theta \qquad (2)$$

During a geomagnetic storm, the impresse field ΔH is positive at the initial phase and negative in the main phase. It is further assumed that the geomagnetic field is confined within a cavity of a certain size. The geomagnetic field beyond this cavity is regarded as a disordered field such that it has no systematic influence upon incoming charged particles. For the initial phase of a storm, the radius of the cavity R_o is defined as the distance where $Hr=0$, viz., $R_o=\left(\frac{\Delta H}{2M}\right)^{-1/3}$. For the main phase, R_o is defined as the distance where $H_\theta=0$, viz., $R_o=\left(\frac{\Delta H}{M}\right)^{-1/3}$. Two models of a magnetic field are shown in Figure 1; (a) represents compression of the geomagnetic field, since there is no line of force across the surface $r=R_o$, and (b) shows the effect of expansion of the geomagnetic field, there by reducing the field intensity near the geomagnetic equator.

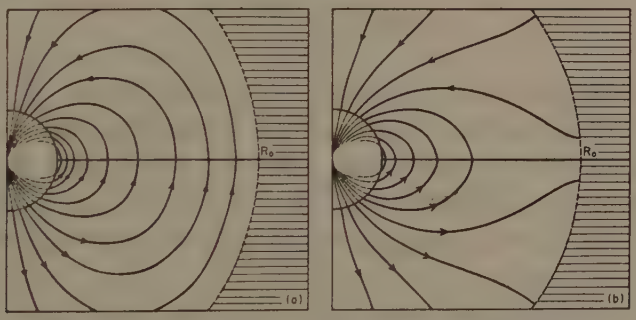

Fig. 1 Two models of distorted geomagnetic fields
a) Model for the initial phase of a geomagnetic storm,
b) Model for the main phase of a geomagnetic storm.

Using these magnetic field models, the cut-off rigidities of incoming particles at various geomagnetic latitudes are computed. The cut-off rigidity of incoming particles P_c at the geomagnetic latitude Φ is given by

$$P_c=\frac{M}{4a^2\gamma^2}\left(1-\frac{\Delta H}{2H_0}\right)^2\cos^4\Phi \qquad (3)$$

where a is the radius of the earth, $H_o=0.31$ *gauss*, and γ is an angular momentum constant, being a complex function of the magnetic field intensity and the particle rigidity.

Results of the computations are shown in Figure 2, where the relation of ΔH and Φ for various cut-off energies of incoming protons is given. It is evident that for the enhanced ΔH——the initial phase of a storm, the zone of particle precipitation shifts

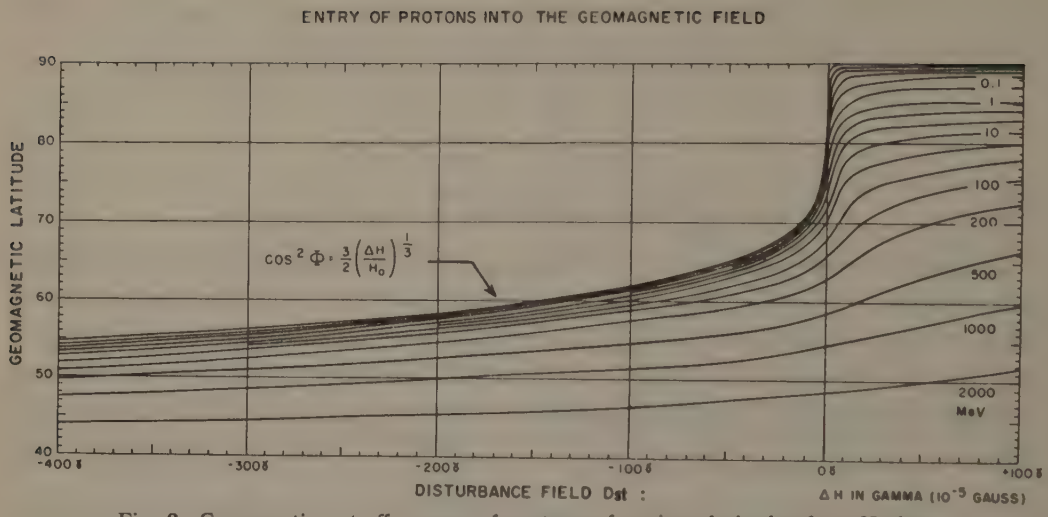

Fig, 2 Geomagntic cut-off energy of protons of various latitudes for ΔH, the Dst field, between $+100\gamma$ and -400γ.

towards high latitudes; while for the depressed ΔH——the main phase, it shifts towards low latitudes. The latitude shift is more pronounced for the lower energy particles than for the higher energy ones. For very low energy particles,

$$\cos^2\Phi = \frac{3}{2}\left|\frac{\Delta H}{H_0}\right|^{1/3}$$

This relation is valid only for the depressed field, and ΔH may be regarded as the Dst-field, the storm-time variation of geomagnetic storms (Chapman and Bartels, 1940).

Since solar cosmic ray particles have a very *steep* energy spectrum, a sharp latitude cut-off exists. Figure 2 is, therefore, useful for the study of such solar cosmic rays, and it is possible to predict a change of the precipitation zone from the observed, Dst-field of a geomagnetic storm.

For the galactic cosmic rays, which have a *shallow* energy spectrum, the diagram shown in Figure 3 is appropriate. The change of cut-off rigidity $\Delta P/P$ versus ΔH is given for different latitudes. Normal cut-off rigidities (for the centered dipole field) are also shown. To determine the change in cosmic ray intensity from the estimated $\Delta P/P$, one may utilize the observed latitude curves of the normal cosmic ray intensity, or else the known rigidity spectrum of the incoming particles. It is shown that for enhanced ΔH——the initial phase of a storm, the cut off rigidity increases and consequently the cosmic ray intensity decreases; while for the depressed ΔH——the main phase, the lowering of the cut-off rigidity results in an increase of cosmic ray intensity. At high latitudes, however, the effect of a geomagnetic storm would be very small, since there is no appreciable latitude variation of the cosmic ray intensity above geomagnetic latitude 50°.

Discussion of the Results

Particles precipitating upon the geomagnetic field behave differently according to

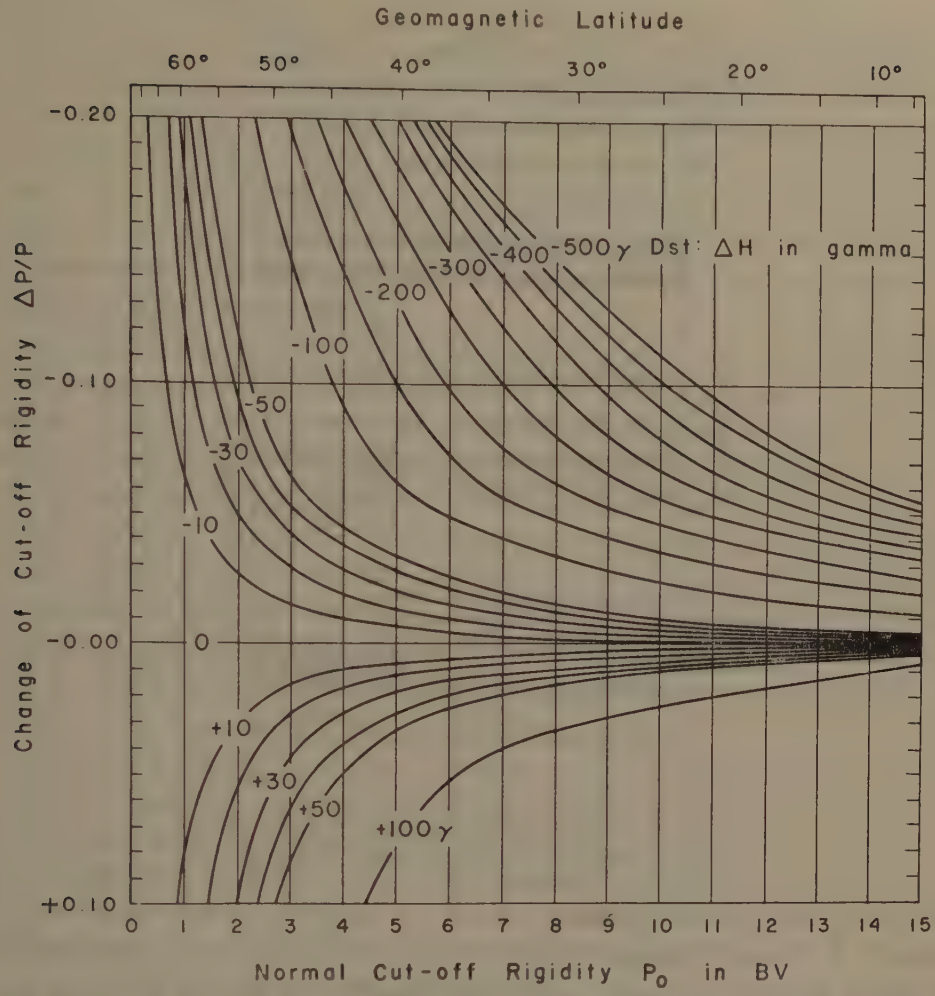

Fig. 3 Change of cut-off rigidity $\Delta P/P$ for various ΔH at different geomagnetic latitudes.

their energy density. It is important to know whether incoming particles behave essentially like a single particle or like a conductive plasma. As has been shown by Ferraro (1952), below a certain critical particle density, the electromagnetic interaction among particles becomes negligible, and their motions may be treated as for a single particle. This criterion can be obtained approximately by equating the shielding depth of a plasma λ_D and the impact parameter of a particle in the geomagnetic field, i. e.,

$$\lambda_D=\sqrt{\frac{mc^2}{8\pi e^2 N}}\geqq\sqrt{\frac{M}{P}} \qquad (4)$$

where N is the particle density and e is the charge in e. s. u. It has been shown elsewhere (Obayashi and Hakura, 1960) that the flux densities of galactic cosmic rays as well as solar cosmic rays above 10–100 Mev are sufficiently low permitting their treatment as single particles. On the other hand, the cloud of low energy particles ejected from the sun behaves like a conductive plasma, and therefore, produces magnetic distortions when it invades the geomagnetic field. Thus, the interesting situation

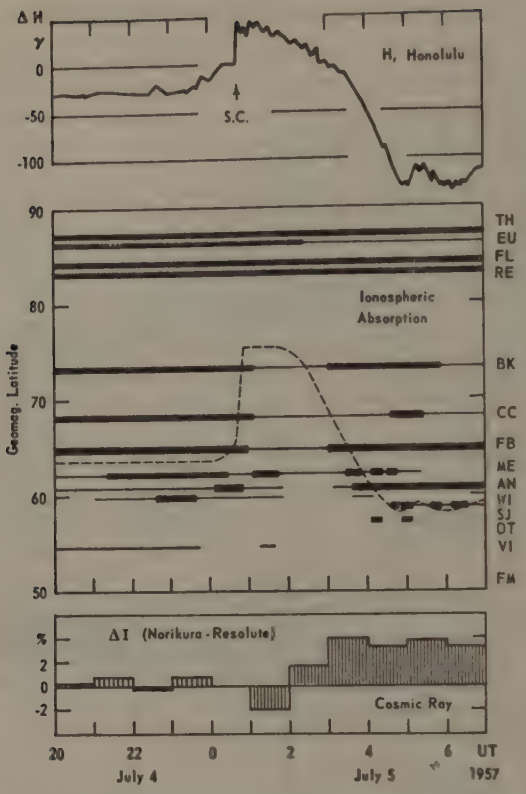

Fig. 4 An example of the geomagnetic storm effect on polar cap absorptions (ionospheric f_{min}) and on galactic cosmic rays.

prevails that although a low energy solar plasma interacts with the geomagnetic field producing a geomagnetic storm, high energy particles penetrate through the distorted geomagnetic field into the upper atmosphere.

A typical example of such a geomagnetic storm effect, for incoming high energy particles, is demonstrated in Figure 4. An intense solar flare, at $08h30m$ on July 3, 1957, produced both a polar cap absorption, that is a solar proton event, and a geomagnetic storm. Enhanced ionization in the polar ionosphere started right after the flare, and the sudden commencement of a storm (SC) occurred 40 hours later at $00h42m$, on July 5. The records are reproduced of the *H*-component of the geomagnetic field at Honolulu, and of the ionospheric absorptions indicated by f_{min} observed at 14 high latitude stations in the northern hemisphere.

The f_{min} data are divided into two degrees; blackouts, indicated by thick line, and The f_{min} above 3 Mc/s, indicated by thin lines. The polar cap blackout developed before the onset of a geomagnetic storm with the southern-most extent approximately 62° N. At the time of the SC, the absorption was reduced suddenly at latitudes below 75° N, and continued until the beginning of the main phase of the storm at $03h30m$ on July 5. The southern-most extent of increased absorption was as low as 58° N during the

main phase of the storm.

Since polar cap blackouts are caused by energetic solar protons precipitating into the polar ionosphere, the observed result is exactly what has been predicted in the present theory. The estimated boundary of precipitating particles of 50 Mev is shown by a dotted line Figure 4. Good agreement exists between the theory and the observational data. Here it has been assumed that even before a geomagnetic storm, the outer geomagnetic field is distorted approximately $\Delta H = -30\gamma$ by interaction between the geomagnetic field and the interplanetary gas, due to the continual orbital motion of the earth (Obayashi, 1959).

A moderate Forbush type decrease of galactic cosmic rays was associated with this geomagnetic storm. The maximum decrease of cosmic ray intensity at high latitudes was approximately 4 per cent. At low latitudes, the decrease was not pronounced, but the intensity appeared to increase slightly during the main phase of the storm. This is also what was expected in the present theory.

In order to see the effect due to geomagnetic distortion, an intensity difference between Mt. Norikura and Resolute Bay is also shown in Figure 4. Since Resolute Bay is situated in the polar cap region where the change of geomagnetic cut-off rigidity barely affects the intensity, this difference represents the net effect due to distortion of the geomagnetic field. It is clear that the galactic cosmic ray intensity decreased slightly at the initial phase, and then increased appreciably during the main phase. Assuming the rigidity spectrum at low latitudes as $P^{-1.5}$, the change in cosmic ray intensity is computed by $\Delta I/I = -1.5 \times \Delta P/P_o$. For the initial phase, $\Delta H \simeq +50\gamma$, the expected decrease is 1.5 percent at Norikura ($\Phi = 25.6^\circ$ N). At the main phase, $\Delta H \simeq -100\gamma$, the increase is approximately 4 per cent, indicating a good agreement with the observed result. Therefore, it seems to be very probable that the storm-time variation of cosmic rays at different phases of a geomagnetic storm can also be explained by the effect of the induced Dst-field.

Thus, independently observed facts concerning the effects of solar cosmic rays and galactic cosmic rays substantiate the present theory. However, some effects cannot be explained by this theory. Occasionally, polar cap absorption events show a definite expansion of the precipitation zone toward the equator at the onset time of geomagnetic storms. It is likely that in these events, energetic particles are trapped in the solar plasma cloud and consequently there is an enormous sudden increase of incoming solar protons upon arrival of the cloud. In such cases, the effect of geomagnetic distortion would be completely masked. Brown et al. (1961) observed a burst of X-rays along the auroral zone at the SC of a geomagnetic storm. They explained this phenomenon as a dumping of electrons from the outer radiation belt. Winckler and his group (1960, 1961) claim that the effect of geomagnetic distortion for solar cosmic rays, viz., a lowering of the cut-off rigidity, is appreciable only during the earlier part of the main phase of a geomagnetic storm. Kellogg and Winckler (1961) has given a tentative explanation of this as the effect of inward shift of the geomagnetic ring current after the main phase of a storm.

Acknowledgements

The major part of the wark was carried out while the author was in residence with Mr. Norman J. Oliver at the Ionospheric Physics Laboratory, Air Force Cambridge Research Laboratories, being sponsored by a U.S. National Science Foundation grant to the Arctic Institute of North America, Grant No. 13840. The author also wishes to express his thanks to Dr. J. R. Winckler for his valuable discussions.

References

Brown, R. R., T. R. Hartz, B. Landmark, H. Leinbach, and J. Ortner, Large-scale electron bombard ment of the atmosphere at the sudden commencement of a geomagnetic storm, J. Geophys. Res., **66**, 1035 (1961).

Chapman, S., and J. Bartels, "Geomagntism", Oxford press, 1940.

Ferraro, V. C. A., On the theory of the first phase of a geomagnetic storm, J. Geophys. Res., **57**, 15, (1952).

Kellogg, P. J. and J. R. Winckler, Cosmic Ray evidence for a ring current, Read at the International Conference on Cosmic Rays and the Earth Storm, Kyoto, Sept. 1961.

Kondo, I., K, Nagashima, S. Yoshida, and M. Wada, On the world-wide cosmic ray intensity increase associated with cosmic ray storms, Proc. Moscow Cosmic Ray Conf. 4. 208 (1960).

Obayashi, T., Entry of high energy particles into the polar ionosphere, Rept. Ionosphere Research Japan, **13**, 201, (1959).

Obayashi, T., and Y. Hakura, Solar corpuscular radiation and polar ionospheric disturbances, J. Geophys. Research, **65**, 3131, (1960).

Obayashi, T., and Y. Hakura, Enhanced ionization in the polar ionosphere associated with geomagnetic storms, J. Atmos. Terr. Phys., **18**, 101 (1961).

Winckler, J. R., and P. D. Bhavsar, Low-energy solar cosmic rays and the geomagnetic storm of May 12, 1959, J. Geophys. Research, **65**, 2637, (1960).

Winckler, J. R., P. D. Bhavsar, and L. Peterson, The time variations of solar cosnic rays during July 1959 at Minneapolis, J. Geophys. Research, **66**, 995, (1961).

Solar Magnetic Cloud Producing Cosmic-Ray Storm, Magnetic Storm and Type IV Solar Radio Outburst

By Yoshiko KAMIYA

Physical Institute, Nagoya University
(Read May 4 1961 ; Received Nov. 7, 1961)

Abstract

Since the discovery of the cosmic-ray storm by Forbush in 1937, the various attempts have been made to explore its nature. Yet its very cause seems to be unclear in view of the lack of phenomena which are intimately correlated with the cosmic-ray storm. In this study the cause of the cosmic-ray storm has been sought after from observed evidences.

In order to find the cause of cosmic-ray storms, the correlation of the spectral type of solar radio outbursts and cosmic-ray variations and magnetic activities has been studied for the data during the period from July 1957 to December 1960. The results obtained are as follows :

(1) Cosmic-ray storms are closely associated with the radio outbursts of Type IV (continuum). The result indicates that the eruption followed by the radio outburst of Type IV is the cause of cosmic-ray storm.

(2) The size of cosmic-ray and magnetic storm was compared with the heriographic longitude of the eruptions. Large magnetic storms occur after eruptions near the central meridian, while the size of cosmic-ray storm is independent of the heliographic longitude of the eruption.

(3) From these results, a possible model of magnetized corpuscular cloud is presented which seems to be ejected from the sun with eruption followed by Type IV outburst. This model of magnetic cloud is a large total bulk with a core and appears to be able to consistently explain not only the facts above described but also the other earth storms.

Introduction

A world-wide decrease of the cosmic-ray intensity accompanied with a magnetic storm was first discovered by Forbush[1] in 1937, and this phenomenon was called the cosmic-ray storm.[2] However, the correlation between the cosmic-ray and the magnetic storm is rather complicated ; large cosmic-ray storms are often associated with very small magnetic storms, while magnetic storms occur without association with cosmic-ray storms. Therefore, it will be difficult to consider that the magnetic storm is a direct cause of the cosmic-ray storm.

In 1953, an interesting statistical study was made by Sekido et al[3]. They classified the magnetic storms into two different types, S-storms and M-storms, respectively ; the S-storms were closely related to sunspot groupes, while the M-storms were not.

They concluded that the former could be attributed to the magnetic corpuscular cloud ejected by solar flares and the latter caused by the non-magnetic corpuscular beams continuously emitted from the solar M-region. This implies that the cosmic-ray storm is caused by something related to sunspots, because magnetic fields should be responsible for modulating cosmic-rays. Actually, however, large flares are not always accompanied by the S-storms. Thus, it is needed to specify the flares by any other factor and to find out the individual correspondence, not statistical, between flares and cosmic-ray storms.

In association with solar flares, on the other hand, there occur outstanding radio outbursts. Paying attention to this fact, we choose those flares which are responsible for the cosmic-ray storms, that is, the flares associated with Type IV radio outbursts, as described in the preceding paper[4]. In fact, a remarkable correlation has been found between cosmic-ray storms and the flares associated with Type IV (continuum) radio outbursts, but the size of the cosmic-ray storm is not always correlated with that of the magnetic storm. This seems to require another parameter which characterizes this correlation.

The individual correlation between cosmic-ray storms and Type IV bursts makes it possible to locate the flare responsible for a cosmic-ray storm. The location of a flare may be a useful parameter which explains the relation between the sizes of the cosmic-ray storm and the magnetic storm.

In the present study, we try (1) to confirm the correlation between cosmic-ray storms and Type IV solar radio outbursts, (2) to find any relation of the sizes of cosmic-ray storms and magnetic storms to the location of responsible flares, (3) to construct, in the light of the evidence presented, a model of the magnetized cloud supposed to be ejected from the sun.

The data used in this paper are as follows: (1) Cosmic-ray data were obtained from the neutron monitor at Mt. Norikura. (2) Solar flare, outburst data were obtaind from Tokyo Astronomical Observatory, Hiraiso Radio Wave Observatory and Harvard spectral data. (3) Geomagnetic data are Kp-index and records at Kakioka Magnetic Observatory.

1. Simultaneous Occurrence of Cosmic-Ray Storm and Type IV Radio Outburst

In the previous paper[4], we have pointed out that during the period of IGY, almost all cosmic-ray storms are associated with the Type IV outbursts. Further examination of available data shown in Table I. confirms this suggestion. Outstanding Type IV bursts were selected from the reports of references (6) (7) and (8), and cosmic-ray storms were defined as variations in which intensity decreases (ΔI) relative to the 27-day running average value were 1 % or more. Magnetic storms were chosen so that they were preceded by Type IV outbursts. Picking up only such cases that two successive storms were well separated in time, we found that in 52 cases among 58 Type IV radio outbursts were followed by the cosmic-ray storms during the period from July 1, 1957 through December 31, 1960. Likewise only of 9 cases among 61

Table 1

Date	Type IV outburst			Flare		Cosmic-ray storm	Magnetic storm	Reference
	Start h m	Duration m	Imp.	Position	Imp.	I %	H	
1957 Jun. 28	0716	70	3	N09, E27	2+	3.0	241	(6)
Jul. 3	0849	25	3	N09, W42	2+	*	155	(6)
16	1801	35	3	S29, W30	2	0.5	90	(6) (8)
24	1802	73	3	S24, W22	3	0.1	52	(6) (8)
Aug. 3	1720		cont. 3	N25, E26	1	2.8	62	(8)
28	0930	75	3	S30, E35	3+	4.8	143	(6)
31	1303	73	3+	N25, W02	3−	*	200	(6)
Sep. 2	1310	60	3+	N11, W26	1+	*	289	(6)
11	0331	91	3+	N11, W03	3	0.4	486	(6)
12	1515	241	3	N11, W19	2+	*	*	(6) (8)
13	1419	97	3			*	*	(8)
26	1948		cont. 2	N24, E27	3	2.8		(8)
Oct. 20	1646	90	3+	S25, W40	3+	5.4	50	(6)
Nov. 24	0903	50	3+	S15, E37	3+	4.6	183	(6)
24	1811	32	3	S12, E23	1	*	*	(6) (8)
Dec. 14	1238	17	3	N18, E77	2+	3.3		(6)
17	0735	31	3+	N22, E44	2	*		(6)
22	1712	56	3	N18, W19	1+	*	49	(8)
1958 Jan. 7	1908	66	3	N30, E48	2	0.8		(8)
20	1453		cont. 2	N28, E28	2	1.6		(8)
Feb. 9	2109	95	3+	S13, W14	2	2.3	617	(6) (8)
Mar. 1	2041	13	3−	S17, W55	1	1.2	83	(8)
23	1002	100	3	S14, E77	3+	3.6	54	(6)
Apr. 25						1.6	40	
May 8	2227		cont. 3	N15, E22	1	1.5		(8)
27	2252		cont. 3	No data		1.6	142	(8)
Jun. 4	2140	36	3	N14, W58	1+	1.1	144	(6)
5	0838	20	3	N27, W65	2+	*	*	(6)
5	1704	24	3	S21, E70	2+	*	*	(6)
6	0434	36	3	N15, W77	2	*	*	(6)
29	2025		cont. 2	N25, E80	1	1.8		(8)
Jul. 7	0027	113	3+	N25, E07	3	2.4	472	(6)
29	0304	57	3+	S14, W43	3	1.6		(6)
Aug. 16	0438	57	3+	S14, W50	3	1.0	198	(6)
19	2316	38	3	N17, E22	1+	*	74	(8)
22	1440	135	3+	N18, W09	3	2.4	120	(6)
26	0019	130	3+	N20, W54	3	*	135	(6) (8)
Sep. 6						0.9		
14	0835	20	3	S11, W80	2	1.3	85	(6)
Oct. 2	1701		cont. 3	N17, E60	2	1.1		(8)
21	2332	18	3+	S03, W22	2	0.8	270	(8)
24	1442	31	3	S04, W58	3	1.5	92	(8)
Nov. 8						2.4	66	
Dec. 12	1415	157	3	S01, W08	2+	1.1	132	(8)
1959 Jan. 6	1715	105	cont. 3			1.0	102	(8)
10	1414	298	cont. 3			*		(8)
22	1547	13	cont. 1,2,3			2.6	114	(8)
Feb. 9	1312	45		N07, E84	2	2.3	176	(6)
9	1400	>188	cont. 3,3+			*		(8)
12	2303	42		N15, E55	3	3.5	99	(6)
Mar. 25	1556	484	cont. 1			2.2	274	(8)
Apr. 7	1505	220	cont. 1			2.0	151	(8)
14	1824	7	cont. 1,2,3			*		(8)
21	1830	1	cont. 3			0.8	160	(8)
May 10	2116	88		N19, E46	3+	4.0	167	(6)
11	2022	20		N08, E39	2+	4.7	109	(6)
Jun. 9	1714	46	cont. 2			0.8	62	(8)
11	0120					1.3		
Jul. 9	2023	110		N14, E67	2	0.7	188	(6)
10	2009	35		N22, E70	3+	*		(6)
14	0338	−100		N17, E06	3	6.8	533	(6)
16	2120	250		N17, W30	3+	9.3	330	(6)
Aug. 14	0140	65		N12, E28	2+	2.9		(6)
18	1029	120		N11, W38	3	*	107	(6)
22	2140	225	2			*		(8)
23	1400	605	3			*		(8)
24	1400	640	3			*		(8)

Table I (continued)

	25	1400	623	3			*		(8)	
	31	1855	30		N10, E11	1+	2.5	166	(6)	(8)
Sep.	1	1914	36	1,2,3			*		(8)	
	19	1912	57	cont. 1,2,3			1.1	118	(8)	
Nov.	30	1750	110	1,2,3			3.6		(8)	
Dec.	1	1400	> 77	2,3			*	156	(8)	
1960 Jan.	6						1.1		(8)	
	11	2105	170	1-3	N23, E03		1.8		(8)	
	12	1653	11	1-2	S10, W37		2.5		(8)	
Feb.	4	2149	11	2-3			1.1		(8)	
	22	1356	20	2	N11, E41		1.2		(8)	
Mar.	28	2051	190	2-3	N11, E39		1.6		(8)	
	29	0000	47	2			2.6		(8)	(7)
	30	1526	454	1-3+	N12, E13		2.8		(8)	
Apr.	29	0208	56	1+	N 9, W20		1.3		(7)	
May	6	1414	118	1-3	S10, E08		3.1		(8)	
	17	1755	34	1-2			0.3		(8)	
	29						1.2		(8)	
Jun.	1	2012	6	1	N18, W90		1.7		(8)	
	25	1215	165	2-3	N22, E06		2.1		(8)	
	25	1717	126	1-3	N19, W01		*		(8)	
	27	0018	31	2-3	S07, E35		*		(8)	
	27	2150	44	3	N23, W23		2.3		(8)	
Jul.	15						1.9		(8)	
Aug.	11	1929	9	1-2	N23, E27		1.0		(8)	
Sep.	3	0038	16	2	N20, E87		0.8		(8)	
	4	0006	22	2			1.6		(8)	
	16	1717	114	1-3+	S21, E66		0.3		(8)	
Oct.	7						1.7		(8)	
	12	1753	6	3	N11, W24		1.2		(8)	
Nov.	12	1345	255	2-3	N27, W01		4.9		(8)	
	19	1636	17	2	N28, W90		1.0		(8)	
	19	1708	15	1-2	N28, W90		*		(8)	
	20	2027	19	2	N25, W90		*		(8)	
Dec.	5	1834	24	3	N30, E90		1.3		(8)	
	14						2.0		(8)	
	26						1.3		(8)	

cosmic-ray storms were not preceded by the Type IV radio outbursts. Since Type IV outbursts and cosmic-ray storms were independently selected, it can be concluded that practically all cosmic-ray storms have nearly one-to-one correspondence with Type IV radio outbursts. The result indicates that the eruption followed by the outburst of Type IV is intimately connected with the cosmic-ray storm.

On the other hand, it was shown, in the previous paper, that during the IGY, Type II (slow drift) outbursts were found to be not associated with cosmic-ray storms. To examine this fact, 69 Type II outbursts with importance 3 or 3+ were selected from the data observed on the Fort Davis records during the period of 1959–1960. From the superposed epoch method about cosmic-ray intensity in which the occurrence of the radio bursts were taken as the zero day, it is shown that there is no significant association between tne cosmic-ray storms and Type II outbursts. On the contrary, Thompson and Maxwell[9] have shown that a statistical association should exist between Type II radio bursts and cosmic-ray storms. Since, however, the Type IV bursts are often preceded by the Type II bursts,[17] the result obtained by these authors seems to be due to the occurrence of a Type IV outburst superposed on Type II.

2. Relation Between the Meridian Distance of the Solar Flares and the Sizes of the Cosmic-Ray and Magnetic Storms

We first examine the heliographic distribution of the flares with Type IV radio outbursts. Figure I shows that those flares with Type IV outbursts followed respectively by cosmic-ray storms and magnetic storms are uniformly distributed over heliographic longitudes.

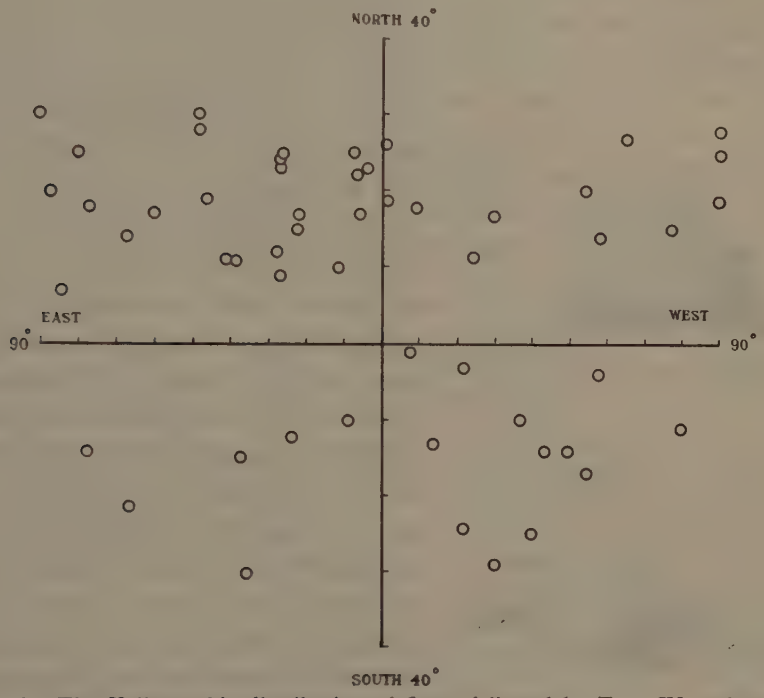

Fig. 1. The Heliographic distribution of flares followed by Type IV outbursts.

In order to study the relation between the meridian distance of the solar flares and the sizes of the cosmic-ray storms and magnetic storms, cosmic-ray storms are classified into three groups according to their size, that is, great storms with $|\Delta I| \geq 4\,\%$, medium storms with $4\,\% > |\Delta I| \geq 2\,\%$ and small storms with $|\Delta I| < 2\,\%$, where ΔI is the difference of the daily mean intensity from the 27-day running average. Magnetic storms are likewise classified into great storms, medium storms and small storms according to $|\Delta H| \geq 300\,\gamma$, $300\,\gamma > |\Delta H| \geq 150\,\gamma$ and $|\Delta H| < 150\,\gamma$, respectively, where ΔH is the maximum range of horizontal intensity during the storm at Kakioka. In order to avoid the ambiguity in deriving the size of decrease, storms having occurred in the recovering periods of preceding ones are excluded. Respective numbers belonging to these classes are listed in Table 2.

The numbers of these events in respective categories against the meridian distances of the positions of corresponding flare are illustrated in Fig. 1 (a) and (b). It is clear that the size of the magnetic storm is strongly dependent on the meridian being re-

Table 2

	Great	Medium	Small
Cosmic-ray	8	17	27
Magnetic Storm	6	14	22

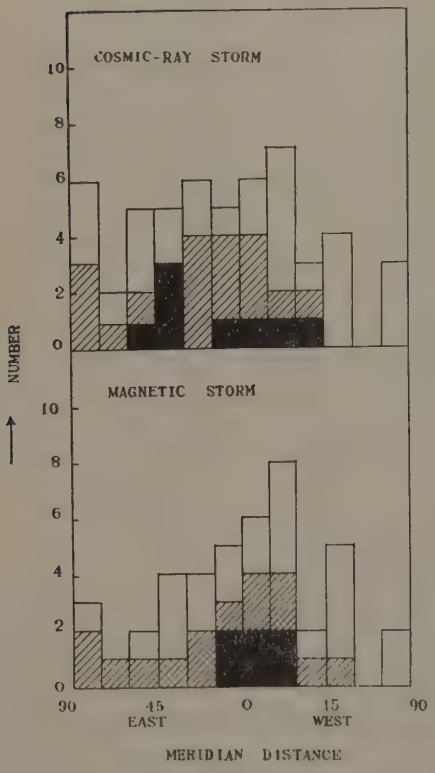

Fig. 2. Dependence of occurrences of cosmic-ray and magnetic storms against the meridian distance of the position of solar flares accompanied by Type IV outburst. The size of cosmic-ray storm is classified as: black ($\geq 4\%$) hatched ($\geq 2\%$) and white ($<2\%$) which are the differences of intensity from 27-day running averaged values, Magnetic storms are classified as: black ($\geq 300\gamma$), hatched ($\geq 150\gamma$) and white ($<150\gamma$) which are the maximum ranges in the storms.

sponsible for larger magnetic storms. On the contrary, the size of the cosmic-ray storm is nearly independent of the position of the corresponding flare. One might be surprised by the fact that the size of cosmic-ray storms caused by the flare occurring near the central meridian is not too large. The reason for this may be explained as follows:

It has been shown by Yoshida and Wada[10] that the world-wide increases of the cosmic-ray intensity occur associated with sever geomagnetic storms, though they are usually superposed on the Forbush type decreases. It is called the storm-time increase. Kondoh et al[11] have given an explanation of this phenomenon as due to the decrease of the cut-off rigidity for incoming cosmic-rays caused by the geomagnetic storm. When a solar flare occurs near the central meridian, a large magnetic storm takes place on the earth and a large *Dst* field thus produced results in a considerable increase of the cosmic-ray intensity at middle and low latitudes. Therefore, the size of the cosmic-ray storm appears to be outwardly small.

3. Model of the Solar Magnetic Cloud Producing the Earth Storm

By way of combining the evidences described above and other results obtained by many authors, a model of the magnetic cloud may be suggested.

Firstly, the terrestrial disturbances caused by a solar flare with Type IV burst are the followings:

(1) Cosmic-ray increase: solar particles of rigidity$>$1 BeV.

(2) Sub Cosmic-ray increase: solar protons ($\sim$100 MeV) inpinging on the upper atmosphere at high latitudes.[12]

(3) Ionospheric disturbance: polar cap blackout (~10 MeV), Type III absorption[14] (~10 MeV) and auroral zone blackout[13] (~1 MeV). When a flare occures in the region of a high magnetic field of a sunspot group, an ionized gas cloud will be ejected outwards from the flare, in which a magnetic field will be frozen, so that high energy particles will be trapped. Type IV outburst is generally believed to be due to the synchrotron radiation from relativistic electrons trapped in this cloud at the corona region. Boischot[16] has already proposed that during this stage, extremely high energy protons could be generated and then might escape along the magnetic line of force to give rise to a terrestrial cosmic-ray increase. This suggestion has been indeed justified even for lower energy protons by the above evidences (1), (2) and (3).

Since it is accepted that cosmic-ray storms are caused by a magnetized cloud, the fact (3) is supposed to be a direct evidence that not only high energy particles but also magnetic clouds are ejected to the interplanetary space from the sun with Type IV burst. By Obayashi and Hakura the relationship among the various disturbances at the time of an earth storm has been classified, as shown in Table 3.

Teble 3 (after T. Obayashi et al)

Type of Combination of Terrestrial Event	Magnetic Storm Type	Cosmic-Ray Storm Type	Combined Type
Type of Radio Outburst	III	IV	IV
Polar Cap Blackout	Absence	Presence	Presence
Auroral Zone Blackout	Presence	Absence	Presence
Magnetic Storm	Typical	Absence	Presence
Cosmic-Ray Storm	Absence	Typical Decrease	Decrease and Increase
Recent Event	Nov. 6, 1957	Oct. 22, 1953	Feb. 11, 1953
Flare Importance	3+	3+	2
Flare Longitude	E 27°	W 40°	W 14°

According to this table, the authors have postulated that there are at least two types of solar corpuscular clouds which are responsible for the earth storm. The cosmic-ray storm type, characterized by the existence of high energy particles of 10～100 Mev, is associated with the Type IV outburst, and the magnetic storm type, consisted of nearly thermal particles, is not, accompanied by the Type IV outburst. These typical two extreme types are, however, rather infrequent but the combined type actually takes place most frequently.

Although these types of the magnetic cloud have been classified according to the conditions at the time of occurrence on the sun, the frequency of the high energy type seems to be too rare to explain the observed facts. Neverthless, it may be possible to explain this by taking account of the structure of the magnetic field that has a core in a large cloud. According to the facts described in the preceding section, if the core invade in the earth field, a rather large geomagnetic storm may be produced

and during its main phase both an auroral zone blackout and a storm-time increase in the cosmic-ray intensity may follow. Then the size of the cosmic-ray storm would not be so large. On the other hand, if the earth will break into the surroundings of the core, no appreciable magnetic storm may occur and consequently no storm-time increase is expected so that the size of cosmic-ray storm would be rather large. The occurrence of the cosmic-ray and sub cosmic-ray increases are independent of whether or not the earth penetrate into the core.

Further details of the structure of the magnetic cloud may be inferred. The core has a considerably regular field which may be ejected from the sunspot field or their neighbourhood and in this field low and high energy corpuscules may be trapped. As far as the low energy corpuscules are concerned the core can be regarded as a dense plasma. The surroundings of the core has a irregular field, diffused from the central regular field, and high energy particles trapped in the core may gradually diffuse into the irregular field, as the cloud is travelling through the interplanetary space. Therefore, the particle density in the outer cloud may be very low. The geomagnetic storm would be produced by rather low energy corpuscules which concentrate in the central core and rather high energy corpuscules expanded in the outer cloud would give rise to the cosmic-ray as well as sub cosmic-ray increases. It seems to us, although not definite, what is essential to the cause of the geomagnetic storm is not the field intensity but the particle density, because as indicated by Sekido et al, even non-magnetic M-region would be able to produce magnetic storms. Hydromagnetic shock front preceding the magnetic cloud will be effective to the sudden commencement of the geomagnetic storm.

It should be noticed that since all cosmic-ray storm are related to flares over the visible hemisphere, the dimension of a magnetic cloud may be of a considerably large scale; its lateral dimension may be considered to be as large as one astronomical unit at the earth's orbit.

Conclusions

In conclusion, the results described in this paper are as follows:

(1) Almost all cosmic-ray storms are closely associated with the radio outbursts of Type IV. It is indicated from this that the eruption followed by the radio outburst of Type IV is the cause of cosmic-ray storm. Evidence has been obtained that the occurrence of a Type IV outburst is a useful event for the prediction of the geomagnetic storm and the cosmic-ray storm commencing 1–3 days later.

(2) According to (1) the location of the eruption producing the cosmic-ray storm has been possible. Therefore, the size of cosmic-ray and magnetic storms were compared with the meridian distance of the eruptions. Large magnetic storms occur after eruptions near the central meridian, while the size of cosmic-ray storms is independent of the meridian distance of the eruption.

(3) From the relationship between the location of the eruption producing the cosmic-ray storm and the size of cosmic-ray and magnetic storm, a possible model of

magnetic cloud has been presented. This model is supposed to explain a series of phonomena in the earth storm.

Acknowlegements

The author wishes to express her sincere thanks to Prof. Y. Sekido and Prof. S. Hayakawa for their valuable discussions and criticisms on this work. She is very grateful to the many investigators who supplied data, in paticular, Dr. U. Hakura of the Hiraiso Radio wave Research Laboratory, Dr. T. Takakura of Tokyo Astronomical Observatory and Dr. A. Maxwell of Radio Astronomy Station of Harvard College Observatory. Her thanks due to Dr. H. Tanaka of Nagoya University Laboratory, Dr. K. Kawabata and Dr. M. Morimoto of Tokyo Astronomical Observatory, Dr. M. Nagai of Kakioka Geomagnetic Observatory and the U.S. Department of Commerce National Bureau of Standards, National committee for the International Geophysical Year Science Council of Japan. Her thanks also due to Dr. M. Wada, Dr. I. Kondō, Dr. S. Yoshida Dr. T. Murayama and Dr. K. Nagashina for their kind advices and encouragements throughout the study.

References

(1) Forbush S.E., Phys. Rev., **51**, 1108, 487, (1937); Phys. Rev., **52**, 1254, 487 (1937).
(2) Sekido Y. Proceedings of the International Conference of Theoretical Physics Kyoto and Tokyo, (1953).
(3) Sekido Y. Wada M. Kondō I. and Kawabata K., Rep. Ionos, Res. Japan, **9**, 174–180 (1955).
(4) Kamiya Y. and Wada M., Rep. Ionos. Space Res. Japan, **13**, 105–111, (1959).; Proceedings of Moscow Conference (1959).
(5) National Committee for the International Geophysical Year Science Council of Japan; Cosmic-ray Intensity during the International Geophysical Year.
(6) Hakura Y. and Goh T. Jour. Radio Research Labo., **6**, No. 28 (1959).
(7) Takakura T, Private communication.
(8) Harvard spectral data in CRPL, Solar Geophysical Data
(9) Thompson A.R. and Maxwell A., Planet Space Sci. **2**, 104–109 (1959).
(10) Yoshida S. and Wada M., Nature **183**, (1959).
(11) Kondō I. Nagashima K. Yoshida S. and Wada M., Proceedings of Moscow Conference (1959).
(12) Ney E.P., Winckler and P.S. Freier, Phys. Rev. (L) **3**, 183 (1959).
(13) Obayashi T. and Hakura Y., Jour. Radio Research Labo, **7**, 27–66 (1960).
(14) Reid G.C. and Leinbach H., J. Geophys. Res. **64**, 1801 (1959).
(15) Sinno K., Rep. Ionos. Res. Japan, **12**, 6–9 (1958).
(16) Boischot and J.F. Denisse, C.R. Acad. Sci., Paris **245**, 2194 (1957).
(17) Mc Lean D.J., Austral. J. Phys. **12**, 404 (1959).

Geomagnetic Secular Variation and Poloidal Magnetic Fields Produced by Convectional Motions in the Earth's Core

By Takesi NAGATA

Geophysical Institute, University of Tokyo

and

Tsuneji RIKITAKE

Earthquake Research Institute, University of Tokyo

(Read November 22, 1961; Received December 1, 1961)

Abstract

A theory of electromagnetic induction by a convectional fluid motion within the earth's core is attempted in the hope of accounting for the localized intense secular variation in the geomagnetic field as has been found in the Antarctic area. If a toroidal magnetic field of 300 gauss at maximum is supposed to exist in the core, a steady convectional motion described by a spherical harmonic of order 5 and degree 5 can give rise to a poloidal magnetic field (degree 6, order 5) of which the Gaussian coefficient of the magnetic potential amounts to 0.045 Γ at the earth's surface provided the radial velocity of the motion is taken as 0.01 cm/sec.

A study of the growth of the field tells us that a secular change of the order of 100 γ/yr is expected as long as a velocity of 0.1 cm/sec is assumed. This order of velocity would not be impossible for such a localized motion as considered here.

1. Introduction

Since Elsasser[1] emphasized the importance of electromagnetic induction within moving material in the earth's core, the possibility of accounting for the non-dipole part of the geomagnetic field and its secular variation through the induction process has drawn attention of a number of authors. For example, Bullard[2] has considered induction in eddies idealized as rotating spheres in order to account for the secular variation observed in South Africa and its neighbourhood. In his result has been suggested an important conclusion that a toroidal field much stronger than the dipole one is likely to be in existence in the core.

Now since IGY, a fairly good network of observations of geomagnetic secular variation has been extended over the whole surface of the earth, and various features of geomagnetic secular variation, especially in the southern hemisphere where only very little had been known until that time, have steadily been clarified. As pointed out and confirmed by one of the present writers[3],[4],[5], a remarkable fact obtained in the recent studies on the secular variation is that an anomalously large secular variation

amounting to about 200 γ/year in rate of change is taking place in the East Antarctic area.

It has been concluded that this large secular variation has continued at least during the past 20 years. The isoporic chart of $\dot{Z}$ for the period of 1955–60 in the southern hemisphere is reproduced in Fig. 1, where the magnitudes of $\dot{X}$ and $\dot{Y}$ are also illustrated by vector arrows.

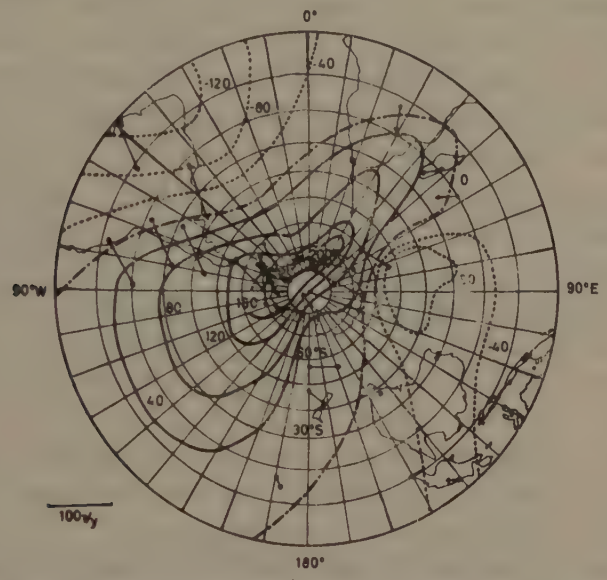

Fig. 1. Isoporic chart of $\dot{Z}$ for 1955–60 in unit of γ/year in the southern hemisphere. Full circles show observing points and arrows represent $\dot{H}=(\dot{X}, \dot{Y})$ at those points.

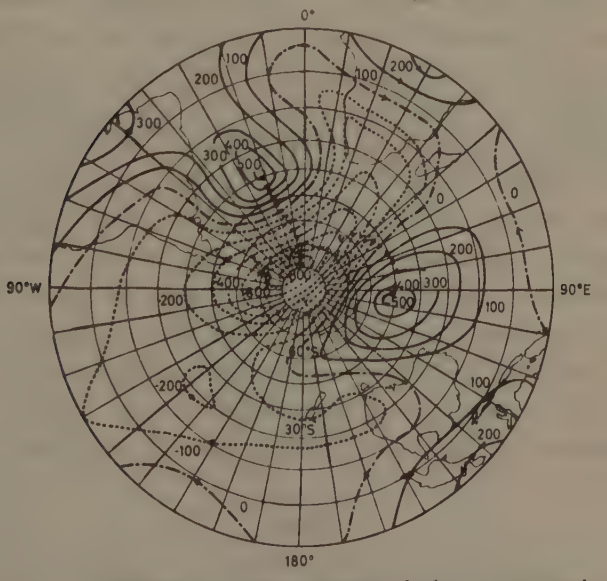

Fig. 2. Equivalent current system of the geomagnetic secular variation at the depth of 2900 km, in unit of 10^4 Ampere/year.

The isoporic chart being subject to a spherical harmonic analysis of 6 in its highest degree, the equivalent current system of the variation assumed at the depth of 2900 km (namely, on the surface of the earth's core) is obtained as illustrated in Fig. 2. As shown in this figure and as confirmed by numerical values of the spherical harmonic coefficients, the localized distribution of the intense secular variation in the Antarctic area can roughly be represented by harmonics of 4, 5 and 6 in their degree.

Then, the question of how such a localized intense secular variation can theoretically be explained may rise again. As a cause of secular variation, the effect of the westward drift of non-dipole components of the geomagnetic field has widely been accepted[6],[7]. Provided that the origin and a sufficiently long life of non-dipole magnetic fields produced in the earth's core are reasonably explained, a possibility of the westward drift of these fields can be theoretically understood[7]. According to the result of analysis, a tendency of westward drift of 0.18 degree/year in average velocity (ranging from 0 to 0.6 degree/year) can be detected for harmonics of $n=2\sim4$, but not for harmonics higher than 4 in their degree. Further, comparing the localized secular variation directly to the non-dipole field[8] in the Antarctic area, it is found that the hypothesis of westward drift of the non-dipole field can not account for the cause of the secular variation.

Then, the most probable theoretical explanation of this phenomenon may be to assume upwelling of a part of strong toroidal magnetic field caused by a particular fluid motion within the earth's core, as already suggested[4].

Bullard's work[2] for interpreting the South African secular variation was along this direction of research. The induction process by rigid rotators embedded in stationary conductors, such as assumed in the Bullard's first paper, has been later examined extensively by Herzenberg and Lowes[9]. In contrast to rigid rotator models, more realistic models based on interaction between magnetic field and fluid motion have been also studied. Coulomb[10] has discussed the advection of the poloidal field on the basis of a simple model for upwelling motion in the core. The idea that a toroidal field which is presumably strong at some depth in the core can be brought up by convection has been discussed by Parker[11]. Although such a distorsion of a toroidal field by convectional motion seems to have an important bearing on the dynamo process which maintains the main geomagnetic field, no exact theory with detailed estimate has been so far available except the work made by Allan and Bullard[12], of which only a short note has been published. It is the intention of this paper to see what the extent of the poloidal field will be outside the core when a fluid motion of convection type and a toroidal field are specified in the core. And it is hoped to find some clue for explaining the intense variation in the Antarctic area.

2. Theory

The induction equation for magnetic field $\vec{h}$ is given by

$$\partial\vec{h}/\partial t-(4\pi\sigma)^{-1}\nabla^2\vec{h}=\mathrm{curl}(\vec{v}\wedge\vec{H}_0) \qquad (1)$$

where σ, $\vec{v}$ and $\vec{H}_0$ denote the electrical conductivity, velocity of the fluid motion and stationary magnetic field. It is not intended here to take the equation of motion into account, so that the present treatment is not really hydromagnetic. Some discussion of the hydromagnetic effect will be made later.

The fluid motion is assumed as a poloidal one. The r, θ and ϕ components of the velocity are given as

$$\vec{v}=\begin{cases}-n(n+1)\xi_n^m(r)r^{n-1}Y_n^m \\ -\left[r\dfrac{d\xi_n^m}{dr}+(n+1)\xi_n^m\right]r^{n-1}\dfrac{\partial Y_n^m}{\partial\theta} \\ -\left[r\dfrac{d\xi_n^m}{dr}+(n+1)\xi_n^m\right]r^{n-1}\dfrac{\partial Y_n^m}{\sin\theta\partial\phi}\end{cases} \qquad (2)$$

where Y_n^m stands for either $P_n^m(\cos\theta)\cos m\phi$ or $P_n^m(\cos\theta)\sin m\phi$ and the origin of the polar coordinate is taken at the centre of the core.

The theory of the origin of the earth's magnetic field suggests that there is a very strong toroidal field, presumably as strong as several hundred gauss, in the core. Let us then assume that the stationary field is given as

$$\vec{H}_0=\begin{cases}0 \\ 0 \\ T_2(r)r^2\dfrac{dP_2}{d\theta}\end{cases} \qquad (3)$$

The induction process due to $\vec{v}$ and $\vec{H}_0$, that is shown by the righthand-side of equation (1), then gives rise to magnetic fields of various types.
They are

Poloidal: S_{n-1}^m, S_{n+1}^m
Toroidal: T_{n-2}^m, T_n^m, T_{n+2}^m

where n and m denote respectively the degree and order of spherical surface harmonics involved. The fields of toroidal type do not appear outside the core provided the conductivity in the mantle is assumed to be very poor, so that our concern is confined to the poloidal ones which are readily written as

S_{n-1}^m field:

$$\vec{h}_{n-1}^m=\begin{cases}-(n-1)n\,s_{n-1}^m(r)r^{n-2}\widetilde{Y}_{n-1}^m \\ -\left[r\dfrac{ds_{n-1}^m}{dr}+ns_{n-1}^m\right]r^{n-2}\dfrac{\partial\widetilde{Y}_{n-1}^m}{\partial\theta} \\ -\left[r\dfrac{ds_{n-1}^m}{dr}+ns_{n-1}^m\right]r^{n-2}\dfrac{\partial\widetilde{Y}_{n-1}^m}{\sin\theta\partial\phi}\end{cases} \qquad (4)$$

S_{n+1}^m field:

$$\vec{h}_{n+1}^m=\begin{cases}-(n+1)(n+2)s_{n+1}^m(r)r^n\widetilde{Y}_{n+1}^m \\ -\left[r\dfrac{ds_{n+1}^m}{dr}+(n+2)s_{n+1}^m\right]r^n\dfrac{\partial\widetilde{Y}_{n+1}^m}{\partial\theta} \\ -\left[r\dfrac{ds_{n+1}^m}{dr}+(n+2)s_{n+1}^m\right]r^n\dfrac{\partial\widetilde{Y}_{n+1}^m}{\sin\theta\partial\phi}\end{cases} \qquad (5)$$

where

$$\widetilde{Y}_n^m = \partial Y_n^m / \partial \phi \tag{6}$$

Introducing (4) and (5) to (1) of which the righthand-side has been calculated from (2) and (3), we obtain differential equations for radial parts s_{n-1}^m and s_{n+1}^m as

$$\frac{d^2 s_{n-1}^m}{dr^2} + \frac{2n}{r}\frac{ds_{n-1}^m}{dr} - k^2 s_{n-1}^m = f_{n-1}(r) \tag{7}$$

$$\frac{d^2 s_{n+1}^m}{dr^2} + \frac{2(n+2)}{r}\frac{ds_{n+1}^m}{dr} - k^2 s_{n+1}^m = f_{n+1}(r) \tag{8}$$

where

$$k^2 = 4\pi\sigma p \tag{9}$$

and p is algebraic operator $\partial/\partial t$. f_{n-1} and f_{n+1} are derived from the induction effect and given as

$$f_{n-1}(r) = -3\frac{n+1}{n-1}\frac{n+m}{2n+1} 4\pi\sigma \xi_n^m(r) T_2(r) r^2 \tag{10}$$

$$f_{n+1}(r) = -3\frac{n}{n+2}\frac{n-m+1}{2n+1} 4\pi\sigma \xi_n^m(r) T_2(r) \tag{11}$$

The solution of differential equation (7), that is finite at $r=0$, is obtained as

$$s_{n-1}^m(r) = r^{-n+1/2}\left[A_{n-1} I_{n-1/2}(kr) + I_{n-1/2}(kr)\int r^{n+1/2} K_{n-1/2}(kr) f_{n-1}(r) dr \right.$$
$$\left. - K_{n-1/2}(kr)\int r^{n+1/2} I_{n-1/2}(kr) f_{n-1}(r) dr\right] \tag{12}$$

in which A_{n-1} is a free constant which is to be determined by the boundary conditions. I and K are modified Bessel functions.

If we ignore the electrical conductivity in the mantle, the potential of the magnetic field corresponding to (4) is given as

$$w_{n-1}^m = a(r/a)^{-n} i_{n-1}^m \widetilde{Y}_{n-1}^m \tag{13}$$

outside the core, where a denotes the core's radius. i_{n-1}^m is then the coefficient for the magnetic potential originating from the interior of the core. The magnetic field is then obtained as

$$\vec{h}_{n-1}^m = \begin{cases} n\left(\dfrac{r}{a}\right)^{-n-1} i_{n-1}^m \widetilde{Y}_{n-1}^m \\ -\left(\dfrac{r}{a}\right)^{-n-1} i_{n-1}^m \dfrac{\partial \widetilde{Y}_n^m}{\partial \theta} \\ -\left(\dfrac{r}{a}\right)^{-n-1} i_{n-1}^m \dfrac{\partial \widetilde{Y}_{n-1}^m}{\sin\theta \partial \phi} \end{cases} \tag{14}$$

At $r=a$, the continuity condition for the normal and tangential components of the magnetic field (the magnetic permeability is assumed as unity in electromagnetic unit) then leads to

$$-(n-1)ns^m_{n-1}(a)a^{n-2}=ni^m_{n-1} \tag{15}$$

$$\left(r\frac{ds^m_{n-1}}{dr}+ns^m_{n-1}\right)_{r=a}a^{n-2}=i^m_{n-1} \tag{16}$$

from which, eliminating i^m_{n-1}, we obtain

$$\left[r\frac{ds^m_{n-1}}{dr}+(2n-1)s^m_{n-1}\right]_{r=a}=0 \tag{17}$$

This is the condition by which constant A_{n-1} is to be determined. Before we proceed to determine A_{n-1}, however, we have to perform the integrations involved in (12). Since no detailed distributions of $\xi^m_n(r)$ and $T_2(r)$ have been so far known, it is necessary to make some assumption concerning these distributions. According to Bullard and Gellman[13], the toroidal field in question is very small at the core-mantle boundary getting larger with the increase in depth. In one of their examples, the maximum of the field intensity occurs somewhere at the depth of $0.4a$. Because of the solid inner core, however, it would seem more likely to suppose that the maximum occurs at a shallower depth.

For the purpose of making the integrals in (12) tractable, it is assumed here that the toroidal field is zero except in a spherical shell between $r=c$ and $r=c+\Delta c$, Δc being small compared to c. $c=0.8a$ and $\Delta c=0.1a$ as chosen in the later numerical work would be one of the likely combinations for actual values. In that case, (12) reduces to

$$s^m_{n-1}(r)=r^{-n+1/2}[A_{n-1}I_{n-1/2}(kr)+c^{n+1/2}\Delta c\bar{f}_{n-1}\{I_{n-1/2}(kr)K_{n-1/2}(kc) -K_{n-1/2}(kr)I_{n-1/2}(kc)\}] \tag{18}$$

where $\bar{f}_{n-1}$ is the mean value of f_{n-1} throughout the shell being approximated by

$$\bar{f}_{n-1}=-3\frac{n+1}{n-1}\frac{n+m}{2n+1}4\pi\sigma\xi^m_n(c)T_2(c)c^2 \tag{19}$$

Going back to condition (17), we may now determine A_{n-1}. We obtain

$$A_{n-1}=-c^{n+1/2}\Delta c\bar{f}_{n-1}[K_{n-1/2}(kc)+I_{n-1/2}(kc)K_{n-3/2}(ka)/I_{n-3/2}(ka)] \tag{20}$$

Putting (20) into (18), $s^m_{n-1}(r)$ is finally solved. In the following, only s^m_{n-1} at $r=a$ is written down as

$$s^m_{n-1}(a)=-\left(\frac{c}{a}\right)^{n-1/2}c\Delta c\bar{f}_{n-1}\frac{1}{ka}\frac{I_{n-1/2}(kc)}{I_{n-3/2}(ka)} \tag{21}$$

With $s^m_{n-1}(a)$ thus determined, (15) enables us to obtain i^m_{n-1}, by which we can estimate the S^m_{n-1} magnetic field emerging through the core's surface.

As for the S^m_{n+1} field, a theory similar to the previous one leads to

$$s^m_{n+1}(a)=-\left(\frac{c}{a}\right)^{n+3/2}c\Delta c\bar{f}_{n+1}\frac{1}{ka}\frac{I_{n+3/2}(kc)}{I_{n+1/2}(ka)} \tag{22}$$

where

$$\bar{f}_{n+1}=-3\frac{n}{n+2}\frac{n-m+1}{2n+1}4\pi\sigma\xi^m_n(c)T_2(c) \tag{23}$$

3. Steady state

Making $p\to 0$ or $k\to 0$, we have

$$I_{n-1/2}(kc)\sim\frac{1}{\Gamma\left(n+\frac{1}{2}\right)}\left(\frac{kc}{2}\right)^{n-1/2}$$

$$I_{n-3/2}(ka)\sim\frac{1}{\Gamma\left(n-\frac{1}{2}\right)}\left(\frac{ka}{2}\right)^{n-3/2}.$$

Putting these into (21), we obtain

$$s^m_{n-1}(a)=-\left(\frac{c}{a}\right)^{2n}a\Delta c\frac{\bar{f}_{n-1}}{2n-1}\qquad\text{for}\quad t\to\infty \tag{24}$$

In the same way, we get

$$s^m_{n+1}(a)=-\left(\frac{c}{a}\right)^{2n+4}a\Delta c\frac{\bar{f}_{n+1}}{2n+3}\qquad\text{for}\quad t\to\infty \tag{25}$$

It is easily seen that solutions (24) and (25) can be directly obtained from differential equations for the steady state.

Now we are in a position to estimate what velocity produces what magnetic field. Let us rewrite (23) as

$$\bar{f}_{n+1}=-\frac{3}{(n+1)(n+2)}\frac{n-m+1}{2n+1}4\pi\sigma\epsilon^{-1}_{n,m}v_r'H_0'c^{-n-1} \tag{26}$$

where v_r' multiplied by $\widetilde{Y}^m_n$ is the r component of the velocity at $r=c$ as given by

$$v_r'=\left[n(n+1)\xi^m_n r^{n-1}\right]_{r=c}\epsilon_{n,m} \tag{27}$$

In numerical work, it is more convenient to make use of spherical functions defined by Schmidt instead of those functions of Neumann's definition which have been adopted in the theory in the last section because, being partly normalized, Schmidt's functions are always less than unity. $\epsilon_{n,m}$ in the above expression is introduced because of the partial normalization and is given by

$$\epsilon_{n,m}=\left\{\frac{(n+m)!}{2(n-m)!}\right\}^{1/2}\qquad\text{for}\quad m\neq 0 \tag{28}$$

Meanwhile, we take

$$H_0'=[T_2r^2]_{r=c} \tag{29}$$

so that, assuming that the maximum value (at $\theta=45°$) of the stationary toroidal field as 300 gauss, H_0' is estimated as 200 gauss.

On the other hand, the coefficient for the S^m_{n+1} field (Schmidt's function is again used) is given by

$$i^m_{n+1}=\frac{3}{n+2}\frac{n-m+1}{(2n+1)(2n+3)}4\pi\sigma v_r'H_0'\Delta c\left(\frac{c}{a}\right)^{n+3}\frac{\epsilon_{n+1,m}}{\epsilon_{n,m}} \tag{30}$$

Suppose that there is a convectional motion of which the velocity is described by $n=5$ and $m=5$. (30) enables us to estimate i_5^5. Let us take

$$\left.\begin{aligned} &\sigma=4\times10^{-6}\ \text{e.m.u.}\\ &\Delta c=0.1a\\ &c=0.8a\\ &a=3470\ \text{km}\end{aligned}\right\} \qquad (31)$$

In that case we see

$$i_{n+1}^m=5.8\Gamma \qquad (32)$$

for

$$v_r'=0.01\ \text{cm/sec} \qquad (33)$$

The Gaussian coefficient of the potential at the earth's surface is then given by $\left(\frac{a}{a_0}\right)^8 i_5^5$ (a_0: the earth's radius) which amounts to 0.045Γ. Judging from the observed magnitude of non-dipole fields, it is therefore possible to suppose that the velocity of the convection motion would be the order of 0.01 cm/sec which has been also suggested by Bullard and Gellman[13] in their theory of geomagnetic dynamo. The induction process considered may well be responsible for the non-dipole fields.

4. Non-steady state

Going back to (21) or (22), which may be regarded as operational equations, we can examine the time-dependent behaviour of the S_{n-1}^m and S_{n+1}^m fields when some sudden change in the velocity takes place. If $\bar{f}_{n-1}$ changes instantaneously at $t=0$ and remains constant afterwards, we obtain

$$s_{n-1}^m(a,\,t)=-\left(\frac{c}{a}\right)^{n-1/2} c\,\Delta c\,\bar{f}_{n-1}\frac{1}{2\pi i}\int_L \frac{1}{\sqrt{4\pi\sigma pa}}\frac{I_{n-1/2}(\sqrt{4\pi\sigma pc})}{I_{n-2/3}(\sqrt{4\pi\sigma pa})}\frac{e^{pt}}{p}dp \qquad \text{for } t>0 \quad (34)$$

where L is Bromwich's path of integration on the complex p-plane.

It is seen that the integrand has a branch point at $p=0$ and simple poles at

$$p=-a_s^2/(4\pi\sigma a^2) \qquad s=1,\ 2,\ 3,\ldots\ldots \qquad (35)$$

while $a_s's$ are the roots of $J_{n-3/2}(z)=0$, so that

$$J_{n-3/2}(a_s)=0 \qquad 0<a_1<a_2<a_3<\ldots\ldots \qquad (36)$$

We take a path of integration as shown in Fig. 3 in which Bromwhich's path of integration is shown by the straight line along the imaginary axis, so that all the singularities lie on the lefthand-side of the path. The branch point and poles are also shown by O, P_1, P_2, P_3,..... . If we further consider the integration along the closed circuit like the one in Fig. 3, we get

$$\int_L=\int_O+\int_{P_1}+\int_{P_2}+\int_{P_3}+\ldots\ldots \qquad (37)$$

where the integrals on the righthand-side are the ones integrated counterclockwise along the small circles centred at O, P_1, P_2, P_3,..... . It is readily proved that the

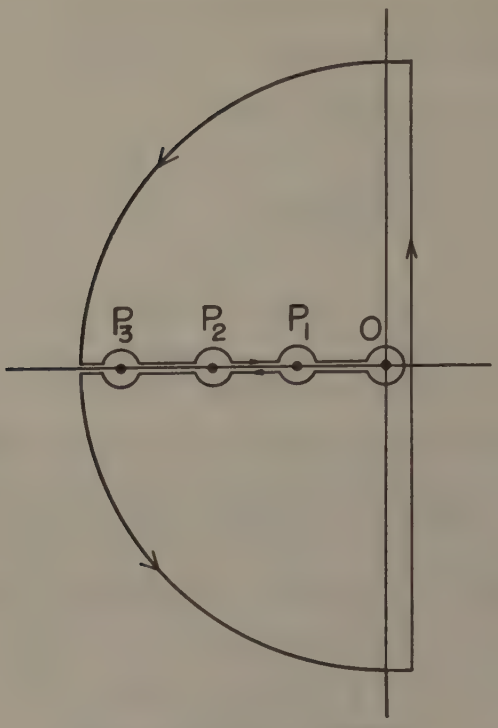

Fig. 3. The path of integration.

integrals along the large semi-circle vanishes when we make the radius infinite. Meanwhile, the integrals along the two straight lines (parallel to the real axis) taken on a Riemann-plane are also proved to cancel one another.

Putting (37), the integrals on its righthand-side being evaluated with the aid of the theory of residues, into (34), we obtain

$$s_{n-1}^{m}(a, t)=F_{n-1}(t)\, s_{n-1}^{m}(a, \infty) \tag{38}$$

where

$$F_{n-1}(t)=1-4(2n-1)\left(\frac{c}{a}\right)^{-n+1/2} \sum_{s=1}^{\infty} \frac{J_{n-1/2}\left(\frac{c}{a}\alpha_s\right)}{J_{n-1/2}(\alpha_s)-J_{n-5/2}(\alpha_s)} \frac{e^{-\frac{\alpha_s^2 t}{4\pi\sigma a^2}}}{\alpha_s^2} \tag{39}$$

In a similar fashion, $s_{n+1}^{m}(a, t)$ is obtained as

$$s_{n+1}^{m}(a, t)=F_{n+1}(t)\, s_{n+1}^{m}(a, \infty) \tag{40}$$

where

$$F_{n+1}(t)=1-4(2n+3)\left(\frac{c}{a}\right)^{-n-3/2} \sum_{s=1}^{\infty} \frac{J_{n+3/2}\left(\frac{c}{a}\beta_s\right)}{J_{n+3/2}(\beta_s)-J_{n-1/2}(\beta_s)} \frac{e^{-\frac{\beta_s^2 t}{4\pi\sigma a^2}}}{\beta_s^2} \tag{41}$$

and

$$J_{n+1/2}(\beta_s)=0 \qquad 0<\beta_1<\beta_2<\beta_3<\cdots\cdots \tag{42}$$

For small values of t, (21) and (22) provide approximate equations like

$$\left.\begin{aligned} s^m_{n-1}(a,\,p) &= -\left(\frac{c}{a}\right)^{n-1/2} c\,\Delta c\,\bar{f}_{n-1}\frac{e^{-k(a-c)}}{ka} \\ s^m_{n+1}(a,\,p) &= -\left(\frac{c}{a}\right)^{n+3/2} c\,\Delta c\,\bar{f}_{n+1}\frac{e^{-k(a-c)}}{ka} \end{aligned}\right\} \qquad (43)$$

so that we obtain

$$\left.\begin{aligned} F_{n-1}(t) &= (2n-1)\left(\frac{c}{a}\right)^{-n+1/2}\left\{\frac{1}{a\pi}\sqrt{\frac{t}{\sigma}}\,e^{-\frac{(a-c)^2\pi\sigma}{t}} - \left(1-\frac{c}{a}\right)\left(1-erf\frac{\sqrt{\pi\sigma}\,(a-c)}{\sqrt{t}}\right)\right\} \\ F_{n+1}(t) &= (2n+3)\left(\frac{c}{a}\right)^{-n-5/2}\left\{\frac{1}{a\pi}\sqrt{\frac{t}{\sigma}}\,e^{-\frac{(a-c)^2\pi\sigma}{t}} - \left(1-\frac{c}{a}\right)\left(1-erf\frac{\sqrt{\pi\sigma}\,(a-c)}{\sqrt{t}}\right)\right\} \end{aligned}\right\} \qquad (44)$$

which are sometimes convenient for numerical work.

Taking $n=5$, for example, the growth of the S^5_6 field is calculated. $F_6(t)$ as obtained from (41) and (44) is illustrated in Fig. 4. We see that the growth of the field is so

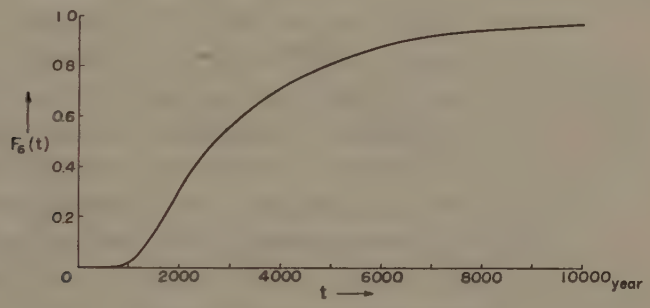

Fig. 4. Growth of the S_6^5 field.

slow in the beginning that no appreciable field is observed until 10^3 years past from the beginning. After that, the rate of increase gets larger, the 70 per cent of the steady field is attained after 4×10^3 years. After 10^4 years, the steady state is nearly reached.

5. Discussion and conclusion

A simple estimate of the time required for transportation of a toroidal field by a motion of fluid, the conductivity of which is so high that the magnetic lines of force are frozen in it, indicates that the time is given by d/v[12] where d is the distance and v is the velocity. In order to bring up the toroidal field from a depth $0.8a$ to the core's surface, it takes only 220 years for a velocity 0.01 cm/sec. From what we have been dealing with in the last section, however, we see that it takes about 1400 years for the S^5_6 field to reach 10 per cent of its steady value. It seems misleading to define the time for the growth of poloidal fields simply by d/v in this case. If transportation is made only by means of diffusion, it would take a time of order $4\pi\sigma d^2$[12] to diffuse from a depth d through material of conductivity σ. Taking $\sigma=3\times10^{-6}$ e.m.u. as before, the time is about 7700 years. The induction process, therefore, seems to give a time for transportation shorter than the one in the case of simple diffusion

process.

The curve in Fig. 4 indicates that the highest rate of increase for the radial component of the S_6^5 field is of the order of $10\,\gamma$/yr at the earth's surface provided a S_6^5 motion having a velocity of the order of 0.01 cm/sec is assumed in the core. If we assume 0.1 cm/sec for the radial velocity, secular change of the order of $100\,\gamma$/yr can be explained. According to the theory of geomagnetic dynamo[13], maximum radial and azimuthal velocities have been estimated as 0.014 cm/sec and 0.04 cm/sec respectively. For a more localized motion, it would not be impossible to suppose a velocity of the order of 0.1 cm/sec, so that the induction model considered here may account for the extremely intense foci of secular variation amounting to $200\,\gamma$/yr at maximum in the Antarctic region.

The theory of induction has been in the above developed by specifying the fluid motion. Physically speaking, however, the driving force rather than fluid motion should have been specified because the pondermotive force produced by the growing magnetic field might become appreciable resulting in a considerable modification of the original motion. Such a dynamical consideration is a matter of great difficulty, no rigorous account based on exact magneto-hydrodynamics has been so far published. Even in this section, a very crude discussion of this point can be made in the following.

Among the various terms of the equation of motion for the core's fluid, it is known that the Coriolis force and the magneto-mechanical forces are the most important[1],[13],[14]. For a nearly steady flow, the magneto-mechanical force is then approximately balanced by the Coriolis force, the magnitude of which is given as $2\omega\rho v$ (ω: angular velocity of the earth's rotation, ρ: density of the core's fluid). Taking $v=0.1\sim0.01$ cm/sec, the Coriolis force and the magneto-mechanical force working on a unit volume of fluid are of order $10^{-4}\sim10^{-5}$ dyn.

The most likely cause of the force that drives the convectional motion is believed to be the buoyancy force which is given as $\rho\alpha g\delta T$, where α is the coefficient of cubical expansion, g is the acceleration of gravity and δT is the temperature departure from the surroundings. Putting $\alpha=4.5\times10^{-6}$ °C^{-1} and $g=800$ cm/sec^2, the buoyancy force becomes $0.04\delta T$ as has been shown by Bullard and Gellman[13]. For the geomagnetic dynamo, it has been also shown by them that there is evidence to suppose that δT is of the order of $10^{-3}\sim10^{-4}$°C, so that the buoyancy force would be of order $10^{-5}\sim10^{-6}$dyn. It would not be also impossible to suppose that δT is a little higher for localized eddies considered in this paper.

Although the estimate above is very crude, we may expect that the pondermotive force produced by the interaction between the induced electric currents and the stationary magnetic field could be of the same order of magnitude as that of the driving force. Since the pondermotive force is directed so as to counteract the fluid motion, the growth of the induced magnetic fields would become prohibited sooner or later because the motion is necessarily slowed down after some time when the pondermotive force is going to overcome the driving force. Whether such a process leads to an oscillation is not clear until a more detailed account of magneto-hydrodynamics becomes

available. The fact that magnetic fields of many types are induced as we have seen in Section 2 makes the situation more difficult.

In the light of the above discussion, it seems doubtful that we have a monotonous approach to the steady state as shown in Fig. 4 in actual cases though the basic idea of induction model would still work in accounting for geomagnetic non-dipole fields and their secular variations.

References

(1) Elsasser, W.M., Phys. Rev., **69**, 106, 1946; **70**, 202, 1947; **72**, 821, 1947.
(2) Bullard, E.C., M.N.R.A.S., Geophys. Suppl., **5**, 248, 1948.
(3) Nagata, T., Oguti, T. and Kakinuma, S., Proc. Japan Acad., **34**, 427, 1958.
(4) Nagata, T., and Syono, Y., J. Geomag. Geoele., **12**, 84, 1960.
(5) Nagata, T., Antarctic Res., No. **11**, 937, 1961.
(6) Bullard, E.C., Freedman, C., Gellman, H. and Nixon, J., Phil. Trans. R.S. London, A, **243**, 67, 1950.
(7) Vestine, E.H., J. Geophys. Res., **58**, 127. 1952.
(8) Nagata, T. and Oguti, T., J. Geomag. Geoelec., (Under Printing).
(9) Herzenberg, A. and Lowes, F.J., Phil. Trans. R.S. London, A, **249**, 507, 1957.
(10) Coulomb, J., Rev. Fac. Sci. Univ. Istanbul, C., **19**, 200, 1954. Ann. Geophys., **11**, 80, 1955.
(11) Parker, E.N., Astrophys. J., **122**, 293, 1955.
(12) Allan, D.W. and Bullard, E.C., Rev. Mod. Phys., **30**, 1087, 1958.
(13) Bullard, E.C. and Gellman, H., Phil. Trans. R.S. London, A, **247**, 213, 1954.
(14) Hide, R., Physics and Chemistry of the Earth 1, p. 94 (Pergamon Press, 1956).

Sound Channel in the Ionosphere

By Yoshihito TAKESADA

Kyoto Gakugei University

(Read November 20, 1961; Received December 29, 1961)

Abstract

The distribution of the sound velocity is obtained by the distribution of the absolute temperature and wind. When the direction of the sound is toward west at the middle latitude, the minimum velocities in summer and winter are estimated to be 210 m/s at 70 km in height and 280 m/s at an altitude of about 90 km respectively. The typical paths of sound waves will be shown by Snell's law in the channel with the axis at these altitudes. The maximum of the sound intensity at an altitude of about 90 km is reduced to about 0.055 dyne/cm^2. The variation quantity of the density which is originated from sound is less than the value of density under the state of equilibrium. When the value of the density-variation reaches about 10^{-8} gm/cm^3 the wave form of the sound will be transformed into the wind at the altitude of about 90 km. During the winter, at the middle latitude, a period of sound waves through the ionosphere comes to about 1 sec, corresponding to wave-length of about 280 m.

1. Introduction

The phenomena of the sound propagation in the upper atmosphere have been investigated by E. Schrödinger, B. Gutenberg and others. In the upper atmosphere, it has been found that the velocity of sound has a minimum at an altitude of about 80 kilometers in accordance with the distribution of temperature only. The propagation velocity of the sound wave is a function of the absolute temperature and affected by wind in the space. In this paper, we will consider the existence of the sound channel in the ionosphere and discuss the intensity and period of the sound in these channels. The main argument of this explanation is based on the results of the following articles, i.e. sound velocity, attenuation of the sound and wind speed in the ionosphere.

The formula of the sound velocity in the upper atmosphere was obtained by M.J. Ference as $T=3.488\times10^{-3}C^2$ (km sec). As to the attenuation of the sound in this altitude, E. Schrödinger introduced the terms of mean free path of the molecule, internal friction and heat conduction. According to the Rocket observation at the middle latitude, the west-component of wind speed at an altitude of 80 km is about 50 m/s in winter.

2. Sound Transmission in the Ionosphere

The transmission of sound waves in the ionosphere is dependent on the vertical distribution of the sound velocity, which is detemined by the temperature and wind. The distributions of temperature and wind speed are given in Figs. (1) and (2). Based on the values of temperature and wind speed, the distribution of the sound velocity is shown in Fig. (3). It is assumed, here, that the direction of sound propagation is

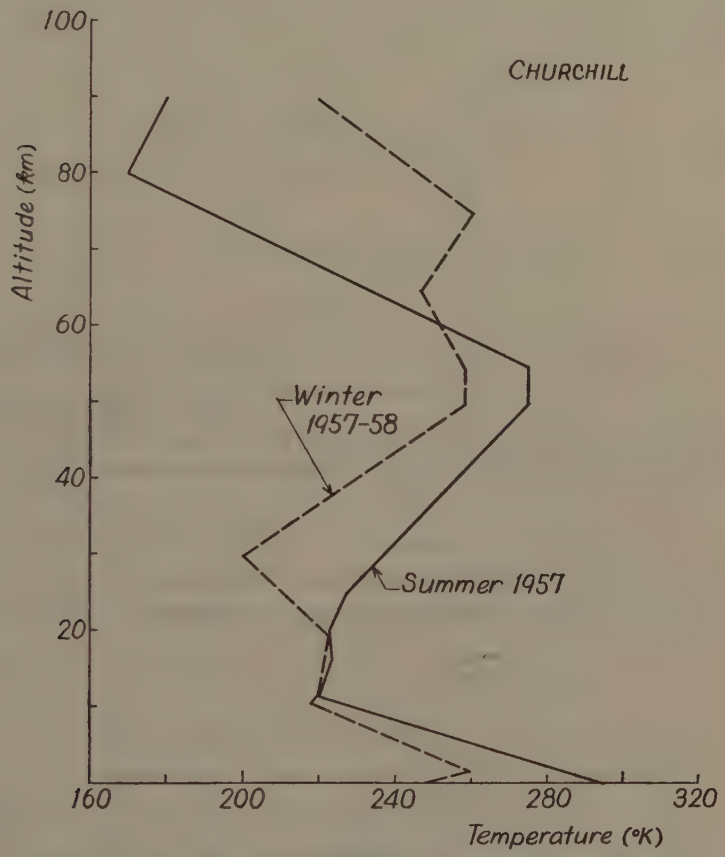

Fig. 1. Temperature distributions in the upper atmosphere. (after W. Nordberg and W.G. Stroud)

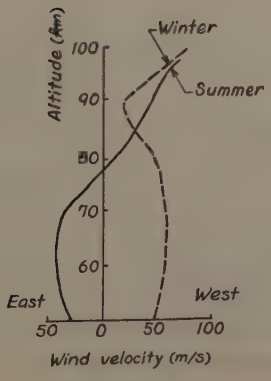

Fig. 2. Wind velocity at the middle latitude. (from Hand Book of Geophys. United States Air Force Geophys. Research Directorate, Chapt. 5, p. 80)

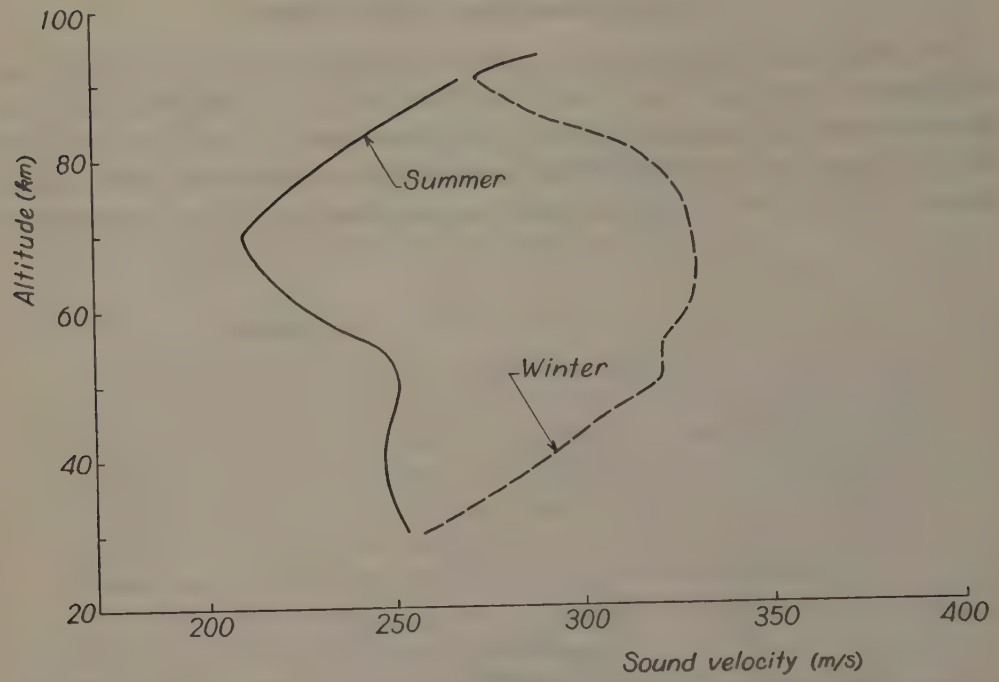

Fig. 3. Distribution of the westward sound velocity in the upper atmosphere. The values of sound velocity is obtained by $C=16.9\sqrt{T}\pm$ (E-W component of wind velocity)

westward and therefore the west component of wind speed adds to the sound velocity.

We can then obtain the mode of the long propagation of the sound wave which depends upon the vertical distribution of the sound velocity. Snell's law, i.e. $\cos\theta=c/c_0$ is used to find ray paths of the infra-sound in the upper atmosphere. It is assumed that the ray path is circular and the velocity C is given by $C=C_0\ (1\pm rZ)$, where $\frac{1}{r}\tan\theta$ is the radius of curvature of the ray, Z is vertical distance from the altitude of the minimum sound velocity and C_0 is the minimum sound velocity. Then r can be obtained as $r=\frac{C_0-C}{ZC_0}$. We can get the path of the sound waves together with the value of radius and the critical angle which is obtained by the ratio of the minimum and the maximum sound velocities.

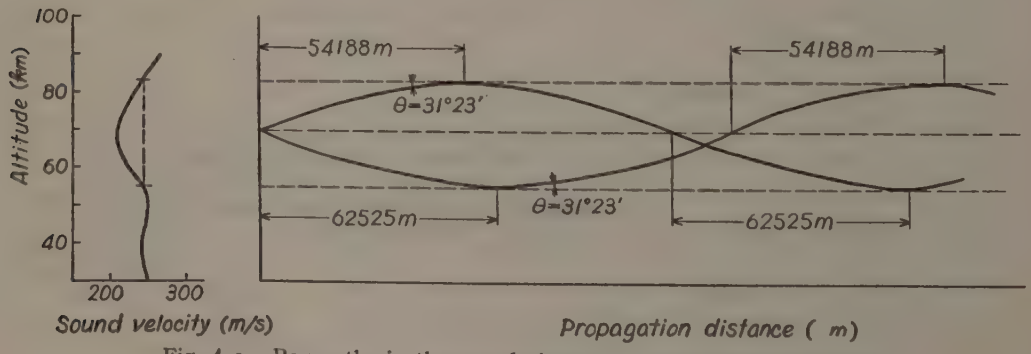

Fig. 4-a. Ray paths in the sound channel of ionospheric *D*-region.

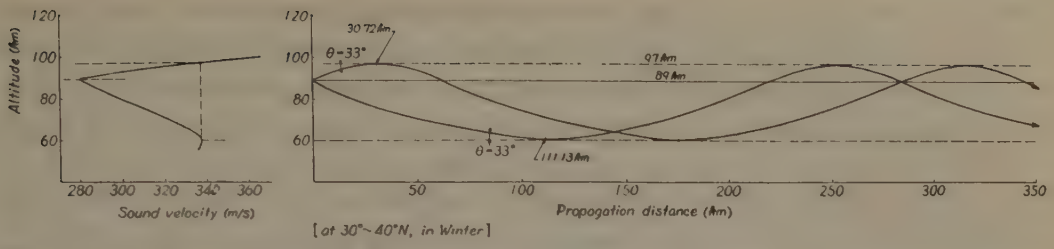

Fig. 4-b. Ray paths through the E-region at the middle latitude in winter. The critical angle $\theta=33°$ and the horizontal distance of the propagation from the source to the apices are 30.72 km and 111.13 km.

The typical paths of sound waves in the upper atmosphere thus obtained by the basic equation of ray acoustic are shown in Figs. 4-a,-b.

3. Sound Intensity in the Ionosphere

The energy of the source in producing sound waves is proportional to the product of acoustic impedance and the square of particle velocity. It is also proportional to the square of the pressure amplitude p. By numerous applications of the above two representations of sound energy and the relation of $C\Delta\rho/\rho_0 \gtreqless \dot{\xi}$ between particles velocity and sound velocity, the relation of $\Delta\rho$ and p are to be found. The intensity of the sound waves will be affected by the density of the medium. The sound waves with infra-frequencies will be transmitted through the ionosphere. The to-and-fro vibrations of the medium are transmitted through the layer with variable sound velocity. As shown in Fig. (5) the value of the density-variation $\Delta\rho$ reaches about 0.055 dyne/cm^2,

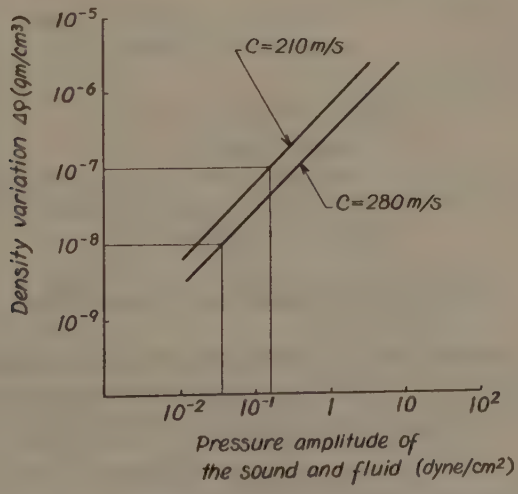

Fig. 5. Relation of the pressure amplitude P and the density-variation $\Delta\rho$ of the sound waves. The maximum intensity of the sound waves at the altitudes with various densities is shown. The curve of larger velocity is arranged on right side.

the wave form of the sound will be transformed into the current of the wind at the altitude of about 90 km. It is possible when the value comes to 0.3 dyne/cm^2, we can see the same phenomenon about 70 km in height. If the pressure amplitude of 0.1 mb is detected on the ground, the sound wave will be not transmitted through the ionosphere. The values of density ρ_0 at the altitude of the axis of sound channel in the upper atmosphere are about 10^{-4} gm/cm^3, 10^{-7} gm/cm^3 and 10^{-8} gm/cm^3 respectively. When the sound occurs in the channels, it will be transmitted with lower density-variation than above mentioned densities.

4. Period of the Sound waves in the Ionosphere

The attenuation at the lower frequencies is smaller for the reason that the absorption constant is proportional to square of frequency. The energy loss rates per km path length in an isothermal atmosphere at an altitude of 70 km are 0.407 and 0.999 at the wave-length of 14 m and 200 m respectively. The rate at 90 km in altitude is shown in Fig. (6) under the condition of temperature of $-45°$C. Attenuation constant is given as $30.1\, l/\lambda^2$ by E. Schrödinger, where l is mean free path of molecules and λ is a wave-length. From the relation of decreasing intensity with the wave-length, possible sound waves which propagate a long distance in the ionosphere is concluded to have larger periods than about 1 sec. If the source of the infra-sound is generated at the neighbourhood of the channel-axis due to the meteors, its part of long periods propagates into the sound channel of the ionosphere in wind direction.

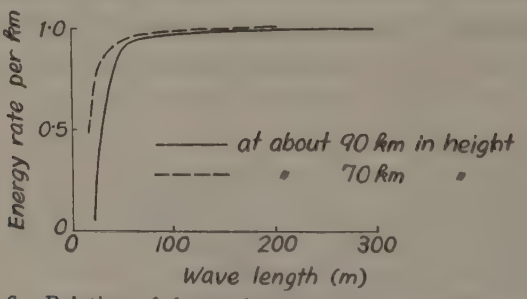

Fig. 6. Relation of decreasing rate of the sound intensity with the wave-length at abont 90 km in height. (after E. Schrödinger)

5. Cloud of the Sound in the Ionosphere

Attenuation of the sound must be small in order that the sound may exist in ionosphere. The propagation of the sound will be made easy by the actual existence of the sound channel. The density of the medium in the ionosphere is rare compared to that at low altitude, so the ordinary sound will disappear quickly. The sound that comes through the rare medium has long wave-length. We can find out the existence of the sound of 1 sec period from the relation of the wave-length of the sound with decreasing energy rate of the sound. The sound which has longer periods than 1 sec will exist easily at these high altitudes. The propagation distance of these sound

waves of the long-period is obtained by the calculation of an attenuation constant. The classical calculation of the absorption constant of the ordinary sound was indicated as $\frac{6.6\times\eta}{\rho_0 C}\cdot\frac{f^2}{C^2}$ by Stokes, were C, η, ρ_0 and f are components of sound velocity, viscosity, density of the medium and frequency of the sound respectively. The formula of Schrödinger corresponds to that of Stokes mentioned above as to the plane wave of the sound. The mean free path of the molecules in connexion with the attenuation constant of the infra-sound in isothermal air was introduced by Schrödinger. The values of l at the standard temperature are about 0.075 cm and 0.7 cm at the altitudes of 70 km and about 90 km respectively according to the table of National Advisory Committee for Aeronautics. For example, if the wave-length are 210 m and 280 m at the altitudes of 70 km and 90 km respectively, i.e. the periods of the sound are 1 sec in both altitudes, the values of the attenuation constant under the standard temperature will be about 5.1×10^{-9} and 2.7×10^{-8} at these altitudes. The decreasing rates of the sound-intensity, and not the intensity of shock waves, for distance of km are shown as the exponential function in Fig. 7. When the infra-sound takes the suitable path in the sound channel, it has the propagation of long distance. When the sources of the sound are created everywhere in the sound channel of E and D-region, the channel is filled with the cloud of the above-mentioned sound. In Fig. 7, the pressureamplitude of the infra-sound at about 200 km distance of travel in E-region is eotimated to be 76% of its amplitude of near the source where it begins to be transformed into sound. The value of this pressure amplitude is about 0.042 dyne/cm^2.

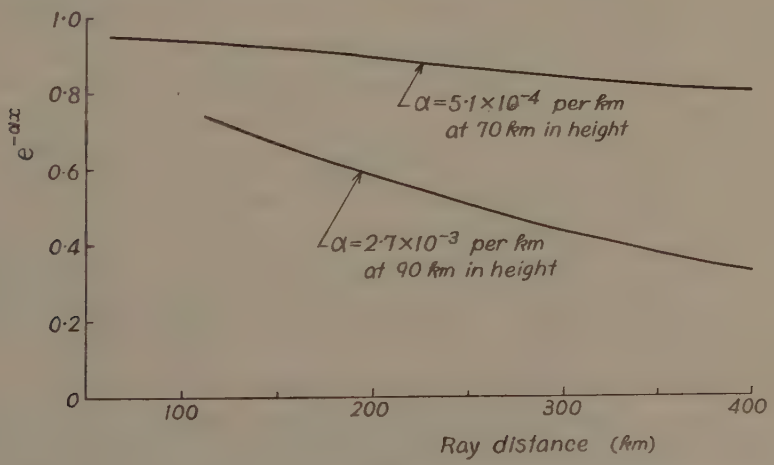

Fig. 7. Decreasing rates of the intensity of infra-sound as plane waves. On the other hand, Spherical waves spread in an infinite homogeneous medium in accordance with the law of inverse squares.

6. Conclusion

The possible axis of the sound channel in the ionosphere is taken to be the altitude of about 70 km and 90 km in summer and winter respectively. It is possible that the density waves in near ionosphere are inhaled into the sound channel. It can be expected

that the sound waves with pressure amplitude of about 0.055 dyne/cm^2 exist at the middle latitude of an altitude of about 90 km. It may be considered that when the sounds of large period exists in above-mentioned channel, of some kinds of geomagnetic variation may occur according to these sound waves. Finally, the author wishes to express his gratitude for the kind advice received from Honorary Prof. Dr. M. Hasegawa and Prof. Dr. M. Ota, University of Kyoto.

References

Schrödinger E: (1917) Phys. Z. 18, 445.
Gutenberg G: (1942) J. Acoust. Soc. Amer., 14, 151.
Nordberg W and Stroud W.G.: (1961) J. Geophys. Research, 66, 463.
Takesada Y: (1961) J. Geomag. Geoelect. 12, 171.

Letter to the Editors

Effect of Solar Cosmic Rays on the Meteorite Radioactivity

In recent papers[1)2)] the spatial distribution of cosmic rays in the interplanetary space has been investigated through the production of radioisotopes in meteorites. Comparing the radioactivity of ^{37}A and that of ^{39}A, Stoenner, Schaeffer and Davis[1)] concluded the spatial constancy of cosmic rays, whereas Fireman and DeFelice[2)] remarked a higher flux at distances closer to the sun. In this note it is pointed out that the contribution of solar particles to the production of radioisotopes which may favour the latter conclusion.

The results of the above two measurements are not much different, as shown in Table 1, but their conclusions are opposite.

Table 1. Ratio of ^{37}A and ^{39}A

	Bombarded by cosmic rays.	Bombarded by protons
Ref. 1.	2.0±0.3	1.5±0.2 (3 GeV)
Ref. 2.	2.3±0.2	1.2±0.3 (2 GeV)

The meteorite used for obtaining the above results is the same, the Hamlet chondritic meteorite which fell on October 13, 1959. About three months before this fall occurred the so-called July 1959 event which consisted of succęssive bursts of intensive solar protons. The integrated proton flux during this event is estimated to be as high as 4×10^8 protons/cm^2 for energies higher than 100 MeV.[3)] This is higher than the Galactic cosmic ray flux during three months.

The amount of ^{37}A of the mean lifetime $\tau=49$ days produced by the irradiation by a constant flux I is proportional to τI, while that by an additional flux ΔI during time T having occurred t days ago is proportional to $\Delta I\cdot T\ \exp(-t/\tau)$. Since I is 2π times the unidirectional intensity, 0.18 cm^{-2} sec^{-1} sterad^{-1},[4)] we have $I\tau\simeq5\times10^7$/cm^2. The intensity of the solar particles at the meteorite, which was located far from the earth at the time of the July event, may be much smaller than that at the earth. Moreover, the steepness of their energy spectrum has to be taken into consideration. It may not be far from reality, on account of the above considerations, if we assume the effective flux of the solar particles responsible for the production of ^{37}A in the meteorite to be about one tenth of the flux at the earth, $\Delta I\cdot T\simeq4\times10^7$/cm^2. Thus we obtain

$$\Delta I\cdot T\ \exp(-t/\tau)/I\tau\simeq7\times10^6/5\times10^7\simeq0.1\,.$$

This estimate does not claim that the ^{37}A/^{39}A ratio of the Hamlet meteorite should be 10% higher than that expected from the constant irradiation, but merely indicates that the contribution of solar particles is so appreciable that the observed results could be interpreted in this way. We would further like to point out that the meteorite

activity gives some information on the propagation of solar particles in a region far from the earth and suggests an experiment for their detection by means of artificial space probes.

By Satio Hayakawa
Physical Institute, Nagoya University.

References

(1) Stoenner, R.W., Schaeffer, O.A. and Davis, Jr. R. (1960) J. Geophys. Res. **65**, 3025.
(2) Fireman, E.L. and DeFelice, J. (1960) ibid, **65**, 3035.
(3) Chupp, E.L. and Williams, R.W. (1961) International Conference on Cosmic Rays and the Earth Storm.
(4) Van Allen, J.A. and Frank, L.A. (1960) Nature **184**, 219.

昭和37年 3 月15日　印刷
昭和37年 3 月31日　發行
第13巻　第1, 2號

編輯兼發行者　日本地球電氣磁氣學會
代表者　永　田　　武

印刷者　京都市南區上鳥羽唐戸町63
田　中　幾　治　郎

賣捌所　丸善株式会社京都支店
丸善株式會社 東京・大阪・名古屋・仙台・福岡

JOURNAL OF GEOMAGNETISM AND GEOELECTRICITY

Vol. XIII No. 1, 2

1961

CONTENTS